

國立台灣大學醫學院分子醫學研究所

碩士論文

Graduate Institute of Molecular Medicine

College of Medicine

National Taiwan University

Master Thesis

果蠅神經樹突中內吞系統的分布及 Nak 調控

Localization and Nak Regulation of Endocytic
Machineries in *Drosophila* da dendrites



Hsien Suo

指導教授：簡正鼎（博士）

Advisor: Cheng-Ting Chien, Ph. D

中華民國 98 年 7 月

July, 2009

摘要

複雜的樹突型態對於神經細胞的正常生理功能是非常重要的。儘管調控樹突發育的細胞機制尚不清楚，但最近已有研究指出外泌系統 (secretory system) 和內吞系統 (endocytic system) 扮演了重要角色。Numb-associated kinase (Nak) 是一個和內吞系統相關的磷酸激酶，並且調控樹突的型態生成。利用核酸干擾技術在果蠅樹狀神經細胞降低 Nak 蛋白的表現量時，會導致樹突分支減少。在過去利用融合螢光蛋白的方式，已經知道 YFP-Nak 會和 Clathrin light chain-GFP 有很好的共位現象，然而，對於 Nak 調控樹突發育的分子機制仍不明瞭。在本篇研究中，我檢驗象徵內吞作用不同路徑的螢光融合蛋白 (包括: Rab4mRFP, Rab5GFP, Rab11GFP 及 ManIIGFP) 在樹突中的數量及分布情形，發現不同的內吞胞器在樹突中會有不同且極性的分布，如: Rab4mRFP 主要位在靠近神經細胞體的樹突中，然而 Rab11GFP 則相反，主要位在遠離細胞體的樹突內。這項結果暗示了不同的樹突區域可能需要不同的內吞系統活性。接著，我發現這些螢光蛋白在樹狀神經的樹突分支點，都和 YFPNak 有相當好的共位現象。然而，當我利用核酸干擾技術抑制 Nak 蛋白表現時，這些螢光蛋白的分布和數量都不受影響。還有，活體影像顯示 YFPNak 和 Rab5GFP 在樹突中具有不同的移動行為。總的來說，本篇研究的實驗數據顯示 Nak 不調控 Rab4mRFP、Rab5GFP、Rab11GFP 及 ManIIGFP 等內吞系統胞器蛋白的數量及極性分布之建立。

Abstract

The great complexity of dendrites is important for their proper functions on receiving and integrating signals. Although the cellular mechanisms regulating dendrite development are largely unknown, secretory and endocytic pathways were recently shown to be involved. Numb-associated kinase (Nak) is an endocytic kinase required for dendrite morphogenesis. Nak depleted da neurons showed decreased numbers of dendritic branches. YFP-Nak is highly co-localized with clathrin light chain (Clc)-GFP at the tips of growing dendrites; however, the molecular mechanisms of Nak in dendrites are still unclear. I am interested in dissecting the endocytic steps that Nak participates in. In this study, I demonstrated the differential distribution of Rab4-mRFP, Rab5-GFP, Rab11-GFP, and ManII-GFP along the dendritic processes, in which Rab4-mRFP and Rab11-GFP preferentially distributed in proximal or distal dendrites, respectively. This data suggest the distinct requirements of cellular activities in different regions of dendrites. Although YFP-Nak colocalized largely with all the examined endocytic markers, knocked-down Nak by RNAi did not exert significant effects on the numbers and distributions of these markers. Moreover, YFP-Nak showed different dynamics with Rab5-GFP and Rab4-mRFP. Collectively, Nak is not functioning in the establishment and maintenance of the polarized distributions of Rab4-mRFP, Rab5-GFP, Rab11-GFP, and ManII-GFP.

目錄

Abstract	iii
目錄	iv
圖目錄	v
Introduction	1
Results.....	9
Differential Occupation of Endocytic Compartments along da Dendrites	9
Colocalizations between YFPNak and Endocytic markers	14
Marker distribution in <i>nak</i> knock-down da dendrites.....	17
Dynamics of YFPNak and Endocytic Markers.....	20
Discussion	22
Highly enriched Rab4mRFP in proximal dendrites.....	22
Differential Requirements of Endocytic Machineries in Different Dendritic Regions.....	23
Dendritic branch points are specialized structures	25
Nak is not involved in the formations and the polar distributions of examined endocytic components	27
YFPNak puncta showed behavioral differences with endocytic markers.....	29
Rab endosomes and motor proteins	30
Materials and Methods	33
<i>Drosophila</i> strains	33
Confocal Imaging.....	33
Live-imaging for trafficking of endocytic markers	33
Scoring of dendritic distribution of endocytic markers.....	34
Measurement of colocalization	34
References	36

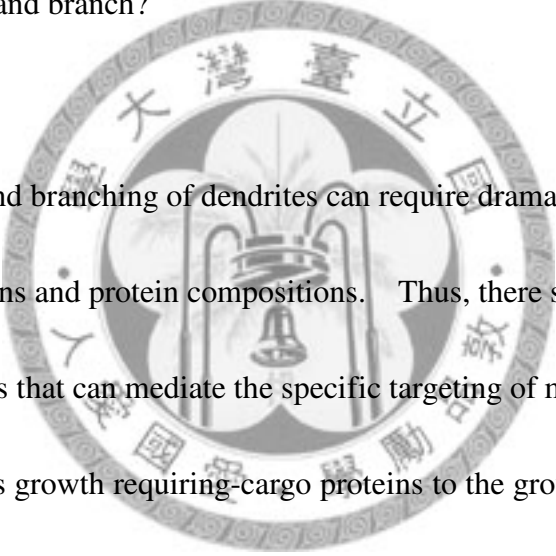
圖目錄

Figure 1. Distributions of endocytic markers in da dendrites.	40
Figure 2. Scoring results of the marker distributions.	42
Figure 3. Rab4mRFP partially colocalized with YFPNak.....	43
Figure 4. Rab5GFP partially colocalized with YFPNak	44
Figure 5. Rab11GFP partially colocalized with YFPNak.....	45
Figure 6. ManIIGFP partially colocalized with YFPNak.....	46
Figure 7. Colocalization status between YFPNak and endocytic compartments.....	47
Figure 8. ClcGFP distribution was dramatically influenced by <i>nak</i> RNAi.....	48
Figure 9. <i>nak</i> depletion globally reduced the puncta number along the dendrites.....	49
Figure 10. Rab4mRFP distribution in dendrites was not altered by <i>nak</i> depletion.....	50
Figure 11. Rab4mRFP puncta number and distribution was not sensitive to Nak level	51
Figure 12. Rab5GFP distribution in dendrites was not altered by <i>nak</i> depletion.....	52
Figure 13. Rab5GFP puncta number and distribution was not sensitive to Nak level.	53
Figure 14. <i>nak</i> depletion did not affect Rab11GFP puncta number and distribution in dendrites	54
Figure 15. The number and distribution of Rab11GFP puncta was not affected in <i>nak</i> depleted neurons	55
Figure 16. ManIIGFP distribution in dendrites was not altered by <i>nak</i> depletion	56
Figure 17. The number and distribution of ManIIGFP puncta was not affected by <i>nak</i> RNAi expression	57
Figure 18. Distribution of Rab4mRFP puncta was not altered by two copies <i>nak</i> RNAi knock-down	58
Figure 19. Distribution of Rab4mRFP puncta was not altered by two copies <i>nak</i> RNAi knock-down	59
Figure 20. Rab5GFP puncta showed dynamic behavior in dendrites	60
Figure 21. Rab4mRFP puncta displayed local motion in proximal dendrites.....	61
Figure 22. YFPNak puncta displayed static behavior in dendrites	62
Appendix 1.	63
Appendix 2	64
Appendix 3	65

Introduction

Neuron is a highly polarized cell type, with the somatodendritic compartment for receiving and integrating upstream signals, and the axonal compartment for transmitting signals. Distinct dendritic branching patterns in different neuronal types are important for their proper functions, and thus must be tightly regulated during development. In fly, dendritic arborization (da) neuron is a group of peripheral multi-dendritic neurons underlying larval epidermis (Grueber, Jan et al. 2002). Da neurons can be divided into four sub-classes according to their branching complexities, from the simplest class I da neurons to the most complex class IV. Class I dendrites are smooth, with few side branches. Class II dendrites are longer than class I and have some high order branches when extending to distal targets. Class III neurons also have long primary and secondary dendrites, but featured in their spiked protrusions along the dendritic shafts and at the ends of main trunks. Class IV neurons have the most extensive branches and the largest dendritic field. The diversity in growth and shape of each class of da neurons has been shown to be regulated by intrinsic cell fate-specifying transcriptional regulators as well as extrinsic guidance cues and dendrite-dendrite interaction-mediated responses (Parrish, Emoto et al. 2007; Corty, Matthews et al. 2009). However, little is known about the cellular activities regulating the dendrite morphogenesis. What are

the down-stream effectors of transcription factors to control dendritic branching and outgrowth? How do dendrites sense and respond to the guidance molecules for their proper innervations? What are the exact cellular mechanisms for dendrites to mediate the contact-dependent regulations, such as self-avoidance and tiling to establish their territories? All the questions above are interesting and largely unsolved. To answer those questions, a fundamental issue must be resolved. That is, mechanistically, how do dendrites elongate and branch?

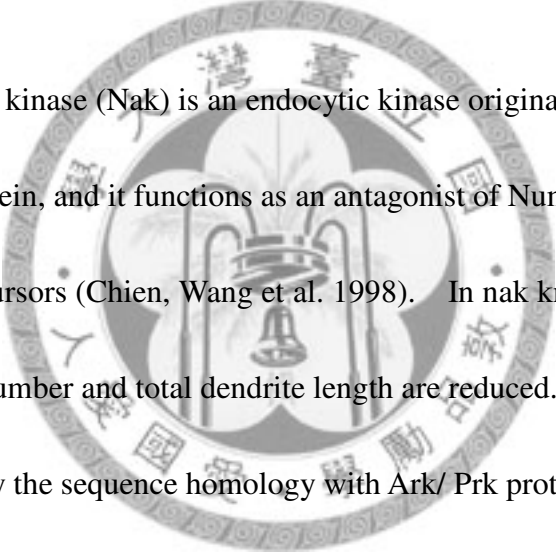


The elongation and branching of dendrites can require dramatic changes in membrane organizations and protein compositions. Thus, there should be polarized trafficking machineries that can mediate the specific targeting of membrane supplements as well as growth requiring-cargo proteins to the growing sites of dendrites. Indeed, the isolated Golgi apparatus, termed Golgi outposts, are shown to be important for proper branching and extension of mammalian as well as invertebrate dendrites(Horton and Ehlers 2003; Horton, Racz et al. 2005; Ye, Zhang et al. 2007). Importantly, limiting ER-to-Golgi transport in *Drosophila* da neurons result in dendritic, but not axonal, growth defects (Ye, Zhang et al. 2007). This distinct reliance of dendrites and axons on the secretory pathway provides a possible mechanism of establishing axon-dendrite polarity. They also found that the Golgi outposts are

distributed primarily in dendrites but little in axons. Moreover, the location of Golgi outposts in dendrites can be correlated with dendritic outgrowth, indicating that the polarized distribution of Golgi outposts is important for their growth-sustaining function (Ye, Zhang et al. 2007). How is this polarized distribution of Golgi outposts and their specific cargos established? A hint came from redistribution Golgi outposts when expressing the dominant-negative form of Lava lamp, a protein involved in the association of Golgi to the dynein complex (Ye, Zhang et al. 2007). More recently, two independent forward genetic screens for mutations that affect the morphology of class IV da neuron identified the mutations in *dynein light intermediate chain (dlic)* that could also cause a proximal shift of dendritic branches (Sato, Sato et al. 2008; Zheng, Wildonger et al. 2008). Importantly, Rab5, the small GTPase involved in early endocytosis, was identified as the interacting protein of Dlic. Rab5 endosomes are lost in the dendrites, but enriched in the soma of *dlic* mutated da neurons (Sato, Sato et al. 2008). Expression of dominant-negative Rab5 in *dlic* mutant neurons can strongly suppress the proximal bushy dendrite phenotype, suggesting the branching-promoting characteristic of Rab5. The mechanisms of Rab5 endosomes to promote dendritic branching is still unknown, however, it may regulate the signal transductions from the membrane receptors uptake (Sato, Sato et al. 2008). Collectively, the vesicle trafficking system has been implicated in the machineries of dendrite growth and

branching, but how the machineries exactly work is still unknown. For example, how are the activities and distributions of Golgi outposts and early endosomes regulated?

Moreover, what are the effectors, or cargos, transported by these polarized trafficking? And how do they function to coordinate dendrite morphogenesis? In addition to the identified Rab5 and Golgi outposts, what are the distributions of other trafficking components and, are they involved in dendrite development?



Numb-associated kinase (Nak) is an endocytic kinase originally identified as a Numb-interacting protein, and it functions as an antagonist of Numb in the development of sensory organ precursors (Chien, Wang et al. 1998). In nak knock-down da neurons, the dendritic branch number and total dendrite length are reduced. Nak has implicated roles in endocytosis by the sequence homology with Ark/ Prk protein kinase family in its N-terminal serine/ threonine kinase domain (Smythe and Ayscough 2003). In yeast, Ark/Prk family proteins are actin regulators involved in endocytosis. For example, Prk1p was proposed to localize around the endocytic vesicles to locally inhibit Pan1p-Arp2/3-dependent actin polymerization, thus enabling the actin to associate with endosomes (Toshima, Toshima et al. 2005). In mammals, Adaptor-associated kinase 1 (AAK1), the human homolog of Nak, can associate with AP2 complex in clathrin-mediated endocytosis (Conner and Schmid 2002). The phosphorylation of $\mu 2$

subunit of the AP2 complex by AAK1 can promote the binding between μ 2 and the sorting signals of cargo proteins. In addition, the efficacy of this phosphorylation is normally low, but strongly enhanced in the presence of clathrin cages, suggesting a tightly regulated kinase activity that can only be activated in the close vicinities of clathrin coated vesicles (Conner, Schroter et al. 2003). Moreover, in the AAK1 RNAi knock-down cells, Transferrin recycling from early endosomes is impaired, suggesting that AAK1 is also involved in endosomal recycling (Henderson and Conner 2007). In da neurons, expression of AAK1 can restore the dendritic-undergrowth phenotype of nak mutant, indicating a functional conservation between human and fly homolog (Peng, Yang et al. 2009). Recently, Nak was reported to be associated with the α subunit of AP-2 complex and the γ subunit of AP-1 complex and regulate the polarized distribution of Dlg, a septate junctional protein, in *Drosophila* salivary gland cells (Peng, Yang et al. 2009). Collectively, Nak is an important regulator and may participate in multiple clathrin-mediated trafficking processes such as early endocytosis and endosomal recycling. What are the functions of Nak in regulating dendrite development? In this study, I am interested in dissecting the endocytic/ recycling steps Nak regulates in controlling da dendrite morphogenesis.

Generally speaking, endosomal network is composed of early endosomes,

recycling endosomes, and lysosomes (Appendix 1)(Kennedy and Ehlers 2006). Newly internalized vesicles take off their clathrin coats and either fusing with each other or with early endosomes. Then the early endosomes are acidified and matured into late endosomes and ultimately fused with lysosomes for degradation. However, if the cargos have to be recycled, they will escape from lysosomal degradation, entering the recycling routes. There are mainly two recycling routes; the first one is to travel from early endosomes to recycling endosomes, and then back to the plasma membrane; the second one also goes from early endosomes to recycling endosomes, however, instead of traveling back to the cell membrane, the cargos are sent to Golgi apparatus, and then traffic along with the secretory pathway. The identities and functions of different endosomal compartments can be determined, at least partially, by the Rab family small GTPases (de Renzis, Sonnichsen et al. 2002). Rab5 localizes and regulates the fusion between endocytic vesicles as well as the fusion between endocytic vesicles and early endosomes. Rab4 is associated with early and recycling endosomes, and is regarded to play a role in fast and continuous recycling events. Rab11 locates at recycling endosomes and mediates the recycling routes to plasma membrane or Golgi apparatus.

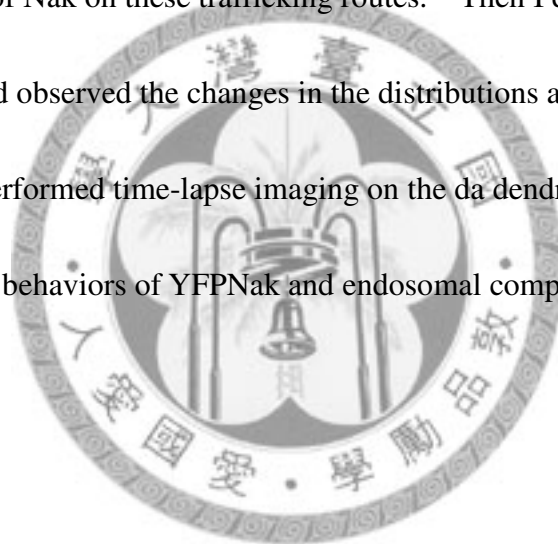
Although the mechanisms of endocytic machineries in regulating dendritic outgrowth are still unclear, there are extensive studies in synaptic plasticity on the dendritic spines in mammalian neuronal cell culture system (Appendix 2) (Newpher and

Ehlers 2008). Rab11-marked recycling endosomes are regarded as the reservoir of AMPA receptor during long-term potentiation (LTP)(Park, Penick et al. 2004). LTP induced by Ca^{2+} influx through NMDA receptors can mobilize the recycling endosomes to move into the spines and insert AMPA receptors into the spine membrane through exocytosis (Park, Salgado et al. 2006; Brown, Correia et al. 2007). Moreover, in LTP, Rab4-dependent constitutive recycling is critical for the maintenance of spine size, albeit it does not influence the transport of receptors (Brown, Correia et al. 2007). However, in long-term depression (LTD), AMPA receptors are endocytosed by a clathrin-, dynamin-, and Rab5-dependent manner, into early endosomes, which in turn transport to late endosomes and subsequent lysosomes for degradation (Brown, Tran et al. 2005). Thus, localization and dynamics of the endocytic system are highly organized in the dendritic spines and are crucial for proper functions of dendrites.

To know the function of Nak, we must know the subcellular localization of Nak. YFPNak was thus made and expressed in da dendrite (Wei-Kan Yang, unpublished), revealed the possible localization of Nak in dendritic branch points and tips. It is not yet clear what other cellular activities also present in the YFPNak positive area. However, the presence of YFPNak is correlated with dendrite elongation, indicating a growth-sustaining role of Nak (Wei-Kan Yang, unpublished). In addition, YFPNak

showed almost perfect colocalization with Clathrin light chain (Clc)-GFP, which suggests Nak may participated in clathrin-dependent trafficking pathways (Wei-Kan Yang, unpublished).

In my study, I characterized the distributions of endocytic machineries in da dendrites by expressing endosomal markers tagged with fluorescent proteins. Also, I examined the colocalizations between YFPNak and those markers to explore the functional relevance of Nak on these trafficking routes. Then I depleted Nak in da neurons by RNAi, and observed the changes in the distributions and numbers of the markers. Finally, I performed time-lapse imaging on the da dendrites of living larva, and demonstrated the behaviors of YFPNak and endosomal compartments.



Results

Differential Occupation of Endocytic Compartments along da Dendrites

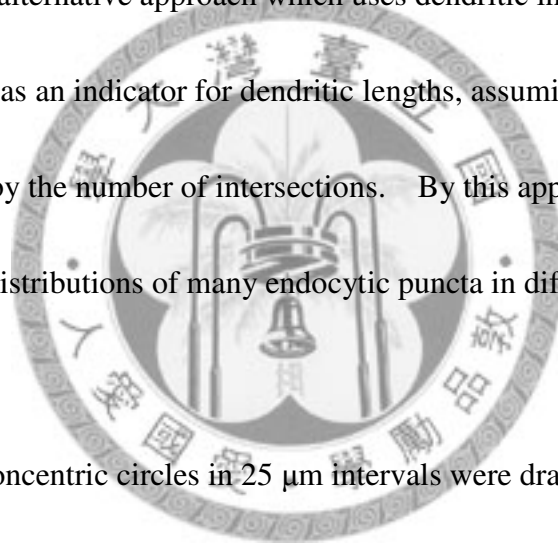
Endocytosis is known to be involved in dendrite growth and spine formation (Brown, Correia et al. 2007; Satoh, Sato et al. 2008). However, the distributions of endocytic compartments in da dendrites during development are still unclear. Moreover, Nak is involved in endocytosis and YFPNak has intriguing localizations at dendritic branch points. To gain more insights into the dendritic locations of endocytosis, I took the advantage of GAL4-UAS system to express Rab4mRFP, Rab5GFP, Rab11GFP, and ManIIIGFP in da dendrites, and examined their distributions individually.

Rab4mRFP is a marker of recycling and early endosomes. When expressed in da neurons by GAL4¹⁰⁹⁽²⁾⁸⁰, Rab4mRFP puncta were localized in the dendritic shafts (Fig. 1A-B, arrows) as well as branch points (Fig. 1A-B, arrowheads). Moreover, Rab4mRFP puncta showed the preference in locating at proximal dendrites (Fig. 1A-B). The straighten dendrite of Rab4mRFP expressing neuron also displayed this proximal-prominent distribution of Rab4mRFP puncta (Fig. 1K). To further elucidate this property of Rab4mRFP, I developed a scoring method to describe and compare the distributions of markers based on the distances between the puncta and the soma.

The ideal indicator of puncta localization preference would be the “puncta

number/unit dendrite length”; the higher of this value could be interpreted as the more possible localization of puncta in the scored dendritic region. So it would be possible to compare the puncta distributional preferences in different regions of dendrites, for example, proximal and distal dendrites. However, the measurement of dendritic lengths is extremely laborious and, in my case, it would be almost impossible to score all the dendritic lengths of da neurons expressing many different endocytic markers.

Thus, I developed an alternative approach which uses dendritic intersections in Sholl analysis (Sholl 1953) as an indicator for dendritic lengths, assuming that the dendritic lengths are reflected by the number of intersections. By this approach, I can efficiently gain insight into the distributions of many endocytic puncta in different dendritic regions.



Practically, 14 concentric circles in 25 μm intervals were drawn with the center at soma, and only the upper hemispheres were scored. The numbers of puncta in each interval of concentric circles were scored manually; also, the Sholl analysis was performed to determine the number of intersections between dendritic branches and circles. To more precisely estimate the dendritic branch numbers *in* the intervals between each pair of concentric circles instead of *on* the circles, the intersection numbers of the two concentric circles defining each interval were averaged. This value was defined as the Dendrite number (Dendrite No.), and I used it to represent the

dendritic branch numbers, and thus dendrite lengths in the space between concentric circles. After all, the final readout of the distributional preferences in each interval of concentric circles was “Puncta number/ Dendrite.” One example for this scoring was shown in a simplified diagram (Fig. 2A). If we want to score the distributional preference of puncta (asterisks) between circle 1 and 2, the puncta number would be 5. The dendrite number would be the average of the numbers of intersections between dendrites and circle 1 and 2, that is, 2 (circle 1 intersection number) plus 3 (circle 2 intersection number), then divided by 2, obtaining Dendrite No. = 2.5. Finally, the readout, puncta number/ dendrite, would be $5/2.5 = 2$.

I scored the distributional preferences of Rab4mRFP puncta in different distances from soma (Fig. 2C, deep red circles). Rab4mRFP occurred with a maximum frequency at about four puncta per branch in the region of 50-75 μm from soma, and then decreased as the distance increases, finally a minimum at less than one puncta per distal branch in the region of 325-350 μm , the most distant region from soma.

Rab5GFP, an early endosomal marker, also localized to the dendritic shafts (Fig. 1C-D, arrows) as well as the branch points (Fig. 1C-D, arrowheads). However, its distribution had little discrimination in dendritic regions, as revealed by the straighten dendrite (Fig. 1L) and the scoring results (Fig. 2C, orange circles).

In contrast, Rab11GFP, the recycling endosomal marker regarded to regulate

long-loop recycling, showed distal-dendrite preference by localizing not only to dendritic shafts (Fig. 1E-F, arrows) and branch points (Fig. 1E-F, arrowheads), but also to dendritic ends of the terminal dendrites (Fig. 1E-F, asterisks). The wider distribution of Rab11GFP along the straightened dendrites (Fig. 1M) could also reflect the scoring of Rab11GFP which showed preferential distribution in distal dendrites (Fig. 2C, yellow triangles). On the other hand, the Golgi resident protein, ManIIIGFP, had less puncta number than Rab4mRFP, Rab5GFP, and Rab11GFP (Fig. 1G, 2D), however, it localized to the dendritic shafts (Fig. 1G-H, arrows) and branch points (Fig. 1G-H, arrowheads) as well. The straighten dendrites (Fig. 1N) and the Puncta no./ Dendrite values (Fig. 2C, green triangles) demonstrated that ManIIIGFP is also distributed equally along the dendritic processes as Rab5GFP does. In addition, YFPNak could also be observed in dendritic shafts (Fig. 1I-J, arrows) and branch points (Fig. 1I-J, arrows). And YFPNak did not display any preference in distributing in proximal or distal dendrites, either, as shown by the straighten dendrite (Fig. 1O) and scoring results (Fig. 2C, indigo squares).

In the straighten dendrites (Fig. 1K-O), we could see that all the examined markers can localized to the branch points, and the differences in distributional preferences were mainly displayed by the small puncta in the dendritic shafts. For example, Rab4mRFP (Fig. 1K) localized to almost every branch points (Fig. 1M, asterisks) just like Rab5GFP

did (Fig. 1L, asterisks), however, Rab4mRFP was highly enriched at the proximal dendritic shaft in the form of small continuous puncta (Fig. 1K, bracket). Moreover, the puncta number varied between markers; Rab4mRFP had the greatest number of puncta per each neuron (Fig. 2D, deep red bar), whereas ManIIIGFP and YFPNak were the least (Fig. 2D, green and indigo bars). By plotting puncta numbers of each interval to their distances from soma (Fig. 2B), the differences in puncta number were reflected by the different heights of the peaks. Rab4mRFP had the highest peak at region 150-175 μm from soma (Fig. 2B, deep red circle), whereas ManIIIGFP (Fig. 2B, green triangle) and YFPNak (Fig. 2B, indigo square) had broad and the lowest peaks at about 150-200 μm from soma. Note that Rab4mRFP, Rab5GFP, and Rab11GFP peaked at different regions of dendrite, with Rab4mRFP peaked at the proximal dendrites (150-175 μm from soma) (Fig. 2B, deep red circle), then Rab5GFP at medial dendritic region (175-200 μm from soma) (Fig. 2B, orange circle), and Rab11GFP peaked at the relatively distal region (200-225 μm from soma) (Fig. 2B, yellow triangle). This differential peaking of endocytic components can partially correlate their preferential distribution revealed by “Puncta No./ Dendrite” in Fig. 2C. Also note that the dendrite numbers of neurons were not dramatically changed by expressing different endocytic markers, as revealed by summing the dendrite numbers of each neuron (Fig. 2E). Together, these data showed a differential distribution and distinct numbers of endocytic

markers, implying the different requirements of distinct endocytic machineries in different dendritic regions. In addition, all the examined endocytic compartments had the common localization at branch points, which suggests that the branch points may be different structures from ordinary dendrites, and may play some special roles that are not yet known.

Colocalizations between YFPNak and Endocytic markers

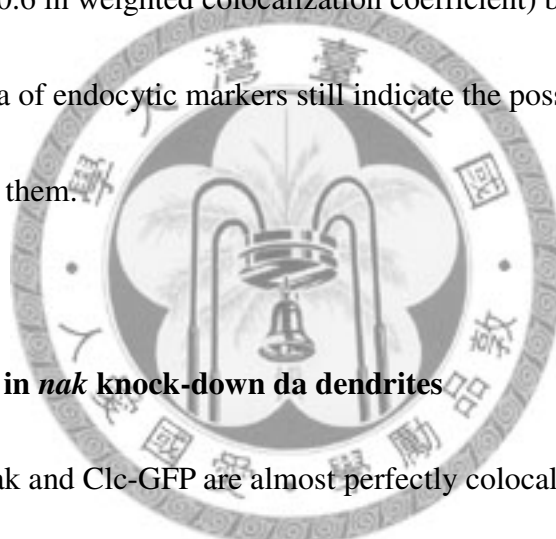
To understand what cellular activities Nak regulates to control dendrite morphogenesis, the colocalizations of YFPNak and Rab4mRFP (Fig. 3), Rab5GFP (Fig. 4), Rab11GFP (Fig. 5), or ManIIIGFP (Fig. 6) were examined. When Rab4mRFP and YFPNak were co-expressed in da neurons, large and bright Rab4mRFP puncta showed good colocalization with YFPNak in the proximal (Fig. 3A-D, arrowheads) and distal dendrites (Fig. 3E-H, arrowheads). However, the smaller Rab4mRFP puncta distributed along the dendritic shaft, mostly, with no YFPNak signal in it (Fig. 3A-H, arrows). Rab5GFP colocalized with YFPNak in proximal (Fig. 4A-D, arrowheads) and distal (Fig. 4E-H, arrowheads) da dendrites, too, although there were still dis-colocalized signals observed (Fig. 4A-H, arrows). Interestingly, Rab11GFP also colocalized with YFPNak in bright-large puncta in proximal (Fig. 5A-D, arrowheads) and distal dendrites (Fig. 5E-H, arrowheads). But similarly, there were dis-colocalized

signals with relatively smaller sizes and weaker intensities (Fig. 5A-H, arrows). On the other hand, the golgi-resident protein, ManIIIGFP, colocalized with YFPNak in proximal (Fig. 6A-D, arrowheads) and distal dendrites (6E-H, arrowheads). Almost all the visible ManIIIGFP puncta were at least partial colocalized with YFPNak, albeit to different degrees.

To compare the colocalization statuses between YFPNak and different endocytic components, I quantified the images for colocalization by a pixel-based (Fig. 7A) as well as an intensity-based (Fig. 7B) method. The pixel-based scoring method calculated the percentage of colocalized pixel number over the total pixel number of YFP channel, and termed as “colocalization coefficient” (Fig. 7A). The intensity-based colocalization parameter was calculated by summing the intensities of colocalized pixels and then over the total intensity of YFP channel (Fig. 7B) thus yielding a percentage. The term “weighted colocalization coefficient” means that the pixels are *weighted* by their intensities in this scoring method. Thus, in the pixel-based “colocalization coefficient”, only the *area* of colocalization was counted (i.e., the larger the colocalized area, the higher coefficient). Whereas in the intensity-based “weighted colocalization coefficient”, not only the *area*, but also the *intensity* were taken into account, that is, the *larger* and *brighter* colocalizing signals contributed more than the smaller and weaker ones on the coefficient.

In the scoring results, pixel-based scoring (Fig. 7A) revealed similar values of colocalization coefficients (about 0.4~0.5) between YFPNak and different endocytic compartments. This result suggests about half of YFPNak positive signals were colocalized with the endocytic markers. However, when intensities were taken into accounts (Fig. 7B), Rab4mRFP (Fig. 7B, deep red bar), Rab11GFP (Fig. 7B, yellow bar), and ManIIIGFP (Fig. 7B, green bar) showed as high as 0.8 in their weighted colocalization coefficient, indicating about 80% of YFPNak intensity units were colocalized with Rab4mRFP, Rab11GFP, and ManIIIGFP. Although slightly lower, Rab5GFP had more than 0.6 in its weighted colocalization coefficient with YFPNak (Fig. 7B, orange bar). The differences in values of weighted and un-weighted colocalization coefficients could be due to the fact that brighter and larger puncta were more likely to be colocalized, whereas the dis-localized puncta were mostly smaller and weaker ones, as demonstrated in Fig. 3-6. The *bright* colocalized puncta can cause the shifts of weighted colocalization coefficients toward higher values than un-weighted colocalization coefficients, because the bright puncta *weighted more* than the dis-localized weak puncta in their intensities, which were not counted in the un-weighted pixel-based scoring parameter. In addition, one may expect that there should be differences in the colocalization statuses between each marker and YFPNak, as suspected by the differential occupation of endocytic compartments along the

dendrites. However, the colocalization statuses did not reflect such differences, neither in pixel-based nor in intensity-based scoring method. This may be due to the strong tendency of colocalization occurrences in the large and bright puncta, thus overwhelming the contributions of smaller dis-colocalized puncta on the coefficients. Thus, my scoring method may not be sensitive enough to discriminate the different colocalizations of YFPNak and small puncta of markers. However, good colocalizations (all > 0.6 in weighted colocalization coefficient) between YFPNak and the bright-large puncta of endocytic markers still indicate the possible functional relationships between them.



Marker distribution in *nak* knock-down da dendrites

In da neurons, YFPNak and Clc-GFP are almost perfectly colocalized with each other (Appendix 3, Wei-Kan Yang, unpublished). Nak knock-down by RNAi led to a dramatic global decrease of Clc-GFP puncta along the da dendrites (Fig. 8, Wei-Kan Yang, unpublished), as well as the significant decrease in dendritic complexity (Fig. 8B and D, Wei-Kan Yang, unpublished). These phenotypes were also reflected by the scoring method developed in this study (Fig. 9). The Clc-GFP puncta number (Fig. 9A; 9D, left two bars) and Puncta number/Dendrite (Fig. 9C) all decreased dramatically along the dendritic processes. The dendrites of *nak* RNAi expressing neuron also decreased

significantly (Fig. 9B; 9D, right two bars), suggesting that the Nak may regulate dendrite development through a clathrin-dependent process. To determine whether Nak is also functionally related to the endocytic components, I used RNAi to knock-down Nak in da neurons, and examined the changes in numbers and distributions of markers.

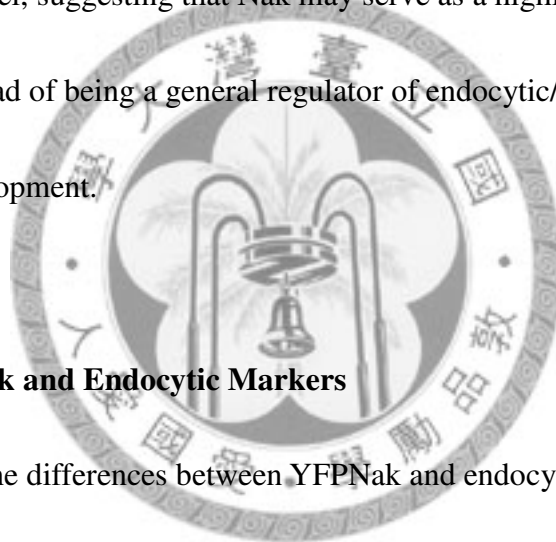
However, *nak* knock-down did not exert any significant effects on either the distributions or numbers of the endocytic markers examined. In Nak depleted da dendrites, the distribution of Rab4mRFP, the recycling and early endosomal marker, was not significantly changed (Fig. 10A-B, LacZ control; C-D, *nak* RNAi), and remained proximal dendritically enriched as revealed by the scoring method (Fig. 11C). The distribution pattern (Fig. 11A) and the total number of puncta (Fig. 11D, left two bars) were not significantly changed. Note that the RNAi expression did not exert strong dendritic loss phenotype in this experiment (Fig. 11B and D). Early endosomal marker Rab5GFP (Fig. 12A-B, LacZ control; C-D, *nak* RNAi) also remained its unbiased distributions along the dendrites in *nak* knocked-down neurons (Fig. 13C). Albeit *nak* RNAi expression cause mild dendritic loss phenotype in high order dendrites (Fig. 12B and D; for statistics, Fig. 13B, and Fig. 13D right two bars), the distribution pattern (Fig. 13A) and the total number (Fig. 13D, left two bars) of Rab5GFP puncta were not altered. Also, recycling endosomal marker Rab11GFP (Fig. 14A-B, LacZ

control; C-D, *nak* RNAi; 15C, statistics) remained distally prominent in *nak* knock-down dendrites, in which the dendrite number was significantly reduced (Fig. 15B and, 15D, right two bars). The distribution pattern (Fig. 15A) and total number (Fig. 15D, left two bars) of Rab11GFP puncta were not altered by *nak* RNAi expression. In addition, the marker of golgi outposts, ManIIIGFP, remained its unbiased distribution along the dendrites in *nak* knocked-down neurons (Fig. 16A-B, LacZ-expressing control; C-D *nak* RNAi; 17C, statistics), note that in this experiment, RNAi expression did not cause significant dendritic loss phenotype. In these experiments, the dendrites of *nak* knocked-down neurons were controlled to display mild or no dendritic loss phenotype, to ensure the possible effects on the distributions of endocytic markers by *nak* depletion were not due to the general disruption of dendritic structures or the sickness of the dendrites.

However, since there were no distributional differences of endocytic compartments observed in the dendrites of LacZ-expressing and *nak* knocked-down neurons, it would be intriguing to examine the distributions of endocytic markers in the dendrites with strong dendritic loss phenotype. Thus, I expressed two copies of *nak* RNAi in *da* neurons to produce severe dendritic loss phenotype, and then examined the dendritic distribution of Rab4mRFP. As expected, when two copies of *nak* RNAi were expressed, dendrites showed severe loss of dendrite numbers (Fig. 18B, 2X LacZ

control; Fig. 18D, 2X *nak* RNAi; for statistics, Fig. 19B, and 19D right two bars).

However, Rab4mRFP remained its proximal preference (Fig. 18A-B, 2X LacZ control; Fig. 18C-D, 2X *nak* RNAi) in *nak* depleted dendrites, and was still enriched in the proximal dendrites, with no significant differences when compared with the control dendrites, which expressed two copies lacZ (Fig. 19C). Collectively, the numbers and distributions of Rab4mRFP, Rab5GFP, Rab11GFP, and ManIIIGFP were not as sensitive as ClcGFP to Nak level, suggesting that Nak may serve as a highly specific regulator of ClcGFP puncta, instead of being a general regulator of endocytic/ recycling trafficking during dendrite development.



Dynamics of YFPNak and Endocytic Markers

To further elucidate the differences between YFPNak and endocytic compartments, I examined the behaviors of Rab5GFP, Rab4mRFP, and YFPNak puncta in living larvae.

The results suggested that Rab5GFP is highly mobile (Fig. 20, arrows), moving relatively fast and long range, although there are still stationary large puncta located primarily at the branch points (Fig. 20, arrowheads). In contrast to the fast and long traveling characteristics of Rab5GFP, Rab4mRFP moved locally (Fig. 21, arrows), either slowly moved back and forth, or split and refused locally, whereas some branch point-localizing Rab4mRFP puncta were stationary (Fig. 21, arrowheads). However,

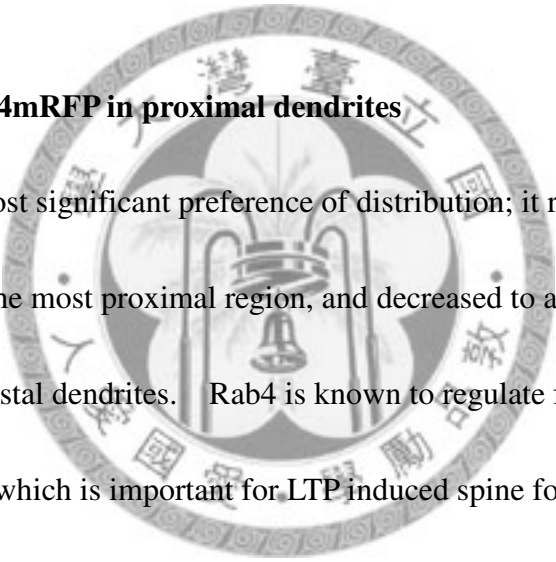
different from the mobile nature of Rab5GFP and Rab4mRFP, all observed YFPNak puncta were relatively stationary, and did not move as the time goes on (Fig. 22, arrowheads). This data demonstrated the different behaviors between YFPNak and endocytic markers.



Discussion

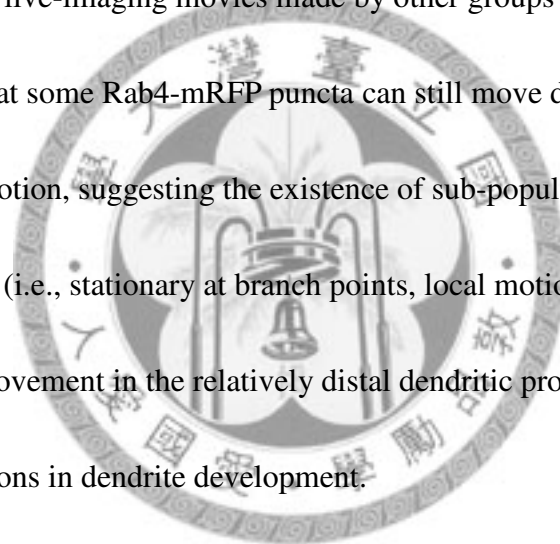
In this study, I demonstrated a differential distribution of endocytic markers in *Drosophila* da dendrites, with Rab4mRFP located proximally, Rab11GFP distally, Rab5GFP and ManIIIGFP equally. Although YFPNak puncta had good colocalizations with these markers, nak RNAi did not affect the distributions of them.

Highly enriched Rab4mRFP in proximal dendrites



Rab4mRFP has the most significant preference of distribution; it ranged from as high as 4 puncta/ dendrite in the most proximal region, and decreased to about only 0.8 puncta/ dendrite in the most distal dendrites. Rab4 is known to regulate fast and continuous endosomal recycling, which is important for LTP induced spine formation: Rab4 is shown to be required for the maintenance of the spine size, although it does not affect AMPA receptor transport (Brown, Correia et al. 2007). It is very interesting that why proximal dendrites contain more Rab4 proteins. One possibility is that the formation and growth of dendritic branches requires dramatic membrane reorganizing, Rab4 may ensure the membrane supplement via its rapid and constitutive recycling function, thereby prevents the membranes to be hijacked by other trafficking pathways. Moreover, usually the proximal dendrites are thicker than the distal ones, so the

reorganization and growth of larger surface membrane may demand more Rab4 activity. That is, Rab4 grab the membranes faster than other membrane trafficking machineries, thus the membrane pool is largely trapped in the Rab4 mediated recycling route, and cycled up and down the dendritic surface very rapidly. My live-imaging data were consistent with this idea, in which Rab4-mRFP puncta only moved locally and may mediate local membrane addition (Fig. 21). However, my later studies (data not shown) as well as the live-imaging movies made by other groups (Stone, Roegiers et al. 2008) also showed that some Rab4-mRFP puncta can still move distantly in da dendrites in addition to local motion, suggesting the existence of sub-populations among all the Rab4-positive puncta (i.e., stationary at branch points, local motion at the vicinities of cell bodies, distant movement in the relatively distal dendritic processes), and may fulfill different functions in dendrite development.



Differential Requirements of Endocytic Machineries in Different Dendritic

Regions

In this study, the endocytic markers displayed different distributions on the distance from cell bodies. Although previous studies in non-neuronal cells have also suggested distinct trafficking routes are regulated by different Rab proteins (de Renzis, Sonnichsen et al. 2002), but this is the first study clearly showed the dramatic difference in

distributions of endocytic components in neurons with a macroscopic view. In non-neuronal cells, the distinct endocytic routes are only few micrometers apart, however, we observed the differences in the sight of hundreds micrometers. Thus, the meaning of this spatial regulation is still unknown. However, in the spines of mammalian dendrites, the spatial regulation of different endocytic compartments is known to be important in synaptic plasticity (Newpher and Ehlers 2008). In addition to Rab4 function in maintaining the spine sizes, Rab11 positive recycling endosomes are regarded as the reservoir of AMPA receptors and moves into dendritic spines during the LTP (Park, Salgado et al. 2006; Brown, Correia et al. 2007). On the other hand, Rab5 was known to regulate LTD-related endocytosis of AMPA receptors, thus facilitating the subsequent degradation of AMPA receptors (Brown, Tran et al. 2005). But again, these different Rab protein-marked endocytic compartments localize near the spines and they apart from each other only in few micrometers. What's the meaning of the macroscopic distributional difference of endocytic compartments in my study and, how is it established, are still open questions. Moreover, one endocytic component may mark different sub-populations of vesicles and/ or compartments, which may exert distinct functions in different dendritic regions. How to do functional studies in local compartments is still a critical issue. Ultimately, the distinct distributions of endocytic components may be the hint for the existence of sub-dendritic compartments, and the

polarity of proximal and distal dendrites; however, the boundaries of these sub-dendritic compartments are still unknown. It will also be interesting to examine how this distal-proximal-dendritic polarity is established.

Dendritic branch points are specialized structures

Although the distributions of endocytic markers were different, the differences are mainly occurred in the small puncta located in dendritic shafts. However, all the examined endocytic markers have good colocalization with YFPNak at the dendritic branch points, in which all the markers as well as YFPNak are highly enriched. That may be the reason why we could see lower colocalizations in the pixel-based scoring method, but much higher colocalizations in the intensity-based scoring method. It is not clear how do these endocytic machineries function in the branch points. In mammalian studies, they have shown that clathrin coated pits and vesicles exist in dendrites and spines (Blanpied, Scott et al. 2002; Cooney, Hurlburt et al. 2002), and the dynamics of clathrin coats is developmentally regulated in an actin dependent manner (Blanpied, Scott et al. 2002). In dendritic spines, clathrin enriches at the region adjacent to the postsynaptic density (PSD), forming a so called “endocytic zone,” which is proposed to undergo fast and local clathrin-mediated recycling of diffused AMPA receptors (Blanpied, Scott et al. 2002; Newpher and Ehlers 2008).

As monitored by clathrin light chain-GFP (Clc-GFP), clathrin is also enriched in the dendritic branch points of da neurons, with almost perfect colocalization with YFPNak. Dendritic branch points thus have very concentrated cellular activities, including endocytic, recycling, and secretory pathways. Golgi outposts and Rab5 endosomes were recently shown to promote dendritic outgrowth and branching and can localize to the branch points (Horton and Ehlers 2003; Horton, Racz et al. 2005; Ye, Zhang et al. 2007; Satoh, Sato et al. 2008). Moreover, the existence of YFPNak, which can also localizes to the branch points, is also correlated with dendrite extension. We do not exactly know that the enrichment of cellular activities at the branch points is established before the branch formation, or is recruited after branch formation. However, because of the time-lapse study of golgi outposts (Ye, Zhang et al. 2007) and YFPNak (Wei-Kan Yang, unpublished) revealed the correlation of the existence of the puncta and dendritic outgrowth, we can imagine that the branch points of mature dendrites were originally the sites of new branch formation during development, thus, it is likely that the endocytic and secretory compartments are recruited to these sites where to form the new branches, and then they sustain the branch formation by their cellular activities. However, are the highly enriched cellular machineries in the branch points of mature dendrites just the vestiges of developmental stages and have little function? We do not know the answer, but the existence of cellular machineries in branch points can serve as

transfer posts for cargos, organizing the transmissions of the signals as well as establishing the polarities and sorting of dendritic proteins in mature neurons.

However, the exact mechanisms of their functions in the branch points to regulate dendrite morphogenesis are still unknown.

Nak is not involved in the formations and the polar distributions of examined endocytic components

Despite of the colocalizations between endocytic components and YFPNak, nak knock-down by RNAi did not affect their puncta numbers and distributions. However, ClcGFP showed global decrease of puncta number under similar RNAi condition.

Thus, the distributions and formations of endocytic components examined in this study are less sensitive to Nak level when compared to ClcGFP. Importantly, the proximal preference and the total puncta number of Rab4mRFP were not altered in the dendrites

of neurons expressing two copies of nak RNAi, which showed strong dendritic loss phenotype (Fig. 18 and 19). This data strongly suggests that Nak is not involved in either the formation of the Rab4mRFP puncta or the establishment of distal-proximal polarity. Notably, in the dendrites bearing two copies nak RNAi, the dendrite number (Fig. 19B, open circles) decreased in the distal dendrites (150-350 μm from soma) as compared to the control, however, slightly but significantly increased in the proximal

dendrites (25-125 μm from soma). This increase may be due to the growth retardation of some dendritic main trunks, causing some crowded and shortened higher order branches to locate in the proximal region, thus displayed a slight increase of dendrite numbers in the proximal region. In addition, the peak of Rab4mRFP puncta localization shifted proximally when compared to the control (Fig. 19A). This suggests that the Rab4mRFP puncta formation was unaffected even when the dendrite outgrowth was significantly disrupted, and the dramatic reduction of distal dendrites may result in the accumulation of Rab4mRFP puncta in the proximal dendrites.

Alternatively, the proximal increase of puncta numbers could be caused by the similar reason as dendrite numbers (proximalized higher order branches may bring the additional Rab4mRFP puncta to the proximal regions). Because of the increase in both proximal puncta and dendrite numbers, the value of “puncta number/ dendrite” was

unaltered. In this case, we can clearly see a draw-back of my scoring method for distribution, that is, the *distance* of the dendrite can not exactly reflect the *order* of dendrites. Even in the normal neurons, the dendrite numbers in every region are

composed of a mixture of high order and low order dendrites, no matter in distal or proximal regions. When the dendrites exhibit strong phenotype, the compositions of

low or high order dendrites in each region are dramatically altered, thus this scoring method may not be the most sensitive way to calculate the distribution. However, this

scoring method is still efficient and sensitive when comparing the dendrites without too severe phenotypes, for example, examining different markers' distributions in the dendrites, or the effect of single copy nak RNAi (which only exert mild dendritic phenotype).

Although Nak seemed not functioned in the formation and the polarized distribution of endocytic compartments, the effect of Nak knock-down on the endocytic markers may be reflected on other aspects instead of distribution. For example, Nak may functionally cooperate with these machineries to regulate dendrite development after the endocytic distributions are already set. The data presented here cannot rule out the possibility that Nak is still functionally related to the endocytic proteins in dendrite morphogenesis. To address that question, the genetic interactions between Nak and endocytic machineries could be done.

YFPNak puncta showed behavioral differences with endocytic markers

In the live-imaging data, YFPNak showed stationary behavior and mainly stayed steadily at branch points. In contrast, Rab5GFP and Rab4mRFP puncta are relatively mobile. However, we also observed Rab5GFP and Rab4mRFP puncta that were constitutively presented in the dendritic branch points, which may indicate the different characteristics of the branch-residing puncta and the traveling puncta. Again, my

live-imaging data suggest that the dendritic branch points are equipped with multiple cellular machineries and may thus serve as specialized structures which are different from the ordinary dendritic shafts..

Rab endosomes and motor proteins

Although we can clearly see that endosomes are dynamic structures which move locally or distantly, the motor proteins carrying these endosomes and the mechanisms regulating the transport are still not clear. In the previous studies, early endosomes have been shown to interact with kinesin-3 family member, KIF16B, in a Rab5 dependent manner, thereby directing the early endosomes to move toward the plus end of microtubules (Nakagawa, Setou et al. 2000). In addition, Rab4 and Rab5 were shown to coordinate the association of early endosomes and dynein motors (Nielsen, Severin et al. 1999; Bielli, Thornqvist et al. 2001). Rab7 recruits dynein to late endosomes via the cooperation with its effector (Jordens, Fernandez-Borja et al. 2001), whereas Rab11 recruits myosin Vb to recycling endosomes (Hales, Vaerman et al. 2002). Moreover, in *Drosophila* da neurons, Rab5 was identified as the dynein interacting protein, and was shown to be transported by dynein motor toward the distal ends of dendrites to control dendritic branching (Satoh, Sato et al. 2008). Because the microtubule orientations in *Drosophila* da neuron are exclusively (~95%) minus end out

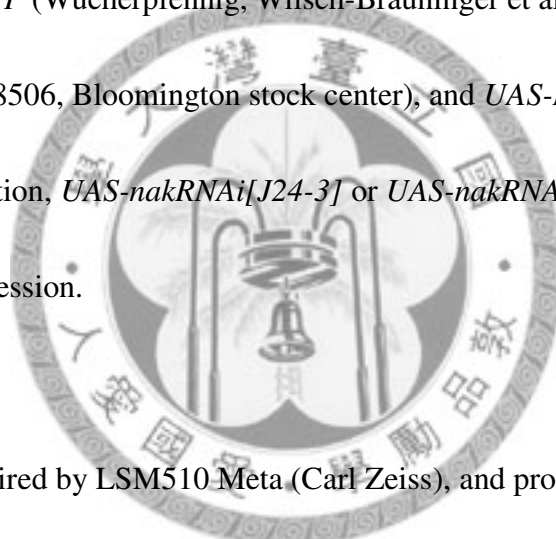
in primary dendrites and mixed orientation (~50%) in the terminal dendrites (Stone, Roegiers et al. 2008), the cargo transport from cell bodies to dendrites relies exclusively on the dynein motors. However, the microtubule orientation between the primary dendrites and terminal dendrites are not known, are they gradually mixed with plus-end out microtubules as the distance from soma increases? Or the microtubules remained exclusively minus end-out orientation until reaching a “critical distance” that the orientations of microtubules suddenly become mixed? In addition, after carrying the cargos to the distal regions of dendrites, dyneins could be transported back to the cell bodies in a kinesin-dependent manner (Sato, Sato et al. 2008), as suggested by the “dynein clumps” observed in *kinesin heavy chain (khc)* mutant dendrites. It would be very interesting to examine the roles motor protein played in the distribution of endocytic compartments. Two possible scenarios could occur, depending on the microtubule organization along the dendritic processes. If the minus end-out microtubules in the primary dendrites gradually mix with plus-end out microtubules as the distance from soma increases, Rab4 endosomes may be transported toward distal region exclusively by dynein, so the distributional density will gradually decreased because of the reduction of minus end-out microtubules. In this scenario, Rab5 endosomes would have to associate with dynein and kinesin motors at the same time, or to exchange their motors between dyneins and kinesins, so that as the Rab5 early

endosomes were transported to the distal regions, they can switch the motor from dyneins to kinesins, thus displaying an unbiased distribution along the entire dendritic process. In addition to the dynein to kinesin switch, Rab11 may recruit myosins as they reach the dendritic ends, thereby associating with actin networks at the dendritic ends to establish the distal preference of Rab11 recycling endosomes. However, in the second scenario, microtubules remained exclusively minus end-out orientation until reaching a “critical distance from soma” or “critical dendritic order” that the orientations of microtubules suddenly become mixed, the distributions of Rab positive endosomes are heavily depends on the balances between dynein motors and kinesin motors, because the plot of “Puncta No./ Dendrite” to “Distance from soma” of Rab4mRFP and Rab11GFP displayed smooth curves instead of a sharp cut-off at certain *distances* from soma. Or it is also possible that the Rab4mRFP and Rab11GFP do exist a sharp cut-off at certain dendritic *orders* (which can not be properly demonstrated by my scoring method), that can correlate with the possible “critical dendritic order” of microtubule orientations. Notably, in both scenarios, there should be at least two populations of kinesin motors, one to transport cargos retrogradely to the cell bodies and the other one to carry cargos anterogradely toward the distal ends of the dendrites. So that the Rab endosomes will be able to transport bi-directionally and in the meanwhile, maintain their specific distal-proximal polarities.

Materials and Methods

***Drosophila* strains**

All flies were fed with standard food and raised at 25°C. In this study, used GAL4 lines were *GALA-109(2)80*, and *ppk-GALA*. UAS lines used to mark dendritic morphologies were *UAS-mCD8GFP*, *UAS-myrmRFP*, and *UAS-mCD8-DSRed*. UAS transgenes of endocytic markers were *UAS-Rab4mRFP* (BL8505, Bloomington stock center), *UAS-Rab5GFP* (Wucherpfennig, Wilsch-Brauninger et al. 2003), *UAS-Rab11GFP* (BL8506, Bloomington stock center), and *UAS-ManIIIGFP* (Ye, Zhang et al. 2007). In addition, *UAS-nakRNAi[J24-3]* or *UAS-nakRNAi[J35-1]* were used to knockdown Nak expression.



Confocal Imaging

All images were acquired by LSM510 Meta (Carl Zeiss), and processed and measured in ImageJ software. Most of the images were acquired by directly mounting late 3rd instar larvae in 87% glycerol, except for the live-imaging images which will be described below. In addition, all the da dendrites examined are dorsal group da neurons.

Live-imaging for trafficking of endocytic markers

Late 2nd or early 3rd instar larvae were anesthetized by PBS containing 40% EtOH and 20% glycerol for about 30 minutes, then mounted in a small drop of halocarbon oil 27

and subjected to confocal scanning. The scanning periods were no longer than 10 minutes to avoid the death of larvae. After image acquisition, larvae were put back to vials with standard foods, only the data from the larvae which can form pupae were shown. The images for Rab5GFP were taken in 1 sec/frame, for YFPNak were about 10 sec/frame.

Scoring of dendritic distribution of endocytic markers

A punctum is defined by at least 3 continuous pixels with intensity larger than 20 (0-255), but because of the higher cytosolic background in proximal dendrites, the punctum was identified by naked eyes based on the morphologies and higher intensities of the signals.

Measurement of colocalization

To measure the colocalizations between endocytic markers and YFPNak, I crop each image with a distal region and a proximal region, in which the thresholds of true signals were determined separately. The thresholds were defined as the intensity values at 20% of the brightest pixel in the cropped images. The “colocalization coefficient” is a pixel based measurement that calculates “colocalized pixel number/ total pixel number of 1 channel.” Thus, for each measurement we could get two values with YFP positive pixel or GFP (or RFP) positive pixel as denominators. However, “weighted colocalization coefficient” takes the intensities of each pixel into consideration. It is

defined by “sum of colocalized intensity of channel A (or B)/ total intensity of channel A (or B)”. Thus there will also be two values, one for YFP, the other for GFP(or RFP) channel.



References

- Bielli, A., P. O. Thornqvist, et al. (2001). "The small GTPase Rab4A interacts with the central region of cytoplasmic dynein light intermediate chain-1." Biochem Biophys Res Commun **281**(5): 1141-53.
- Blanpied, T. A., D. B. Scott, et al. (2002). "Dynamics and regulation of clathrin coats at specialized endocytic zones of dendrites and spines." Neuron **36**(3): 435-449.
- Brown, T. C., S. S. Correia, et al. (2007). "Functional compartmentalization of endosomal trafficking for the synaptic delivery of AMPA receptors during long-term potentiation." Journal of Neuroscience **27**: 13311-13315.
- Brown, T. C., I. C. Tran, et al. (2005). "NMDA receptor-dependent activation of the small GTPase Rab5 drives the removal of synaptic AMPA receptors during hippocampal LTD." Neuron **45**(1): 81-94.
- Chien, C. T., S. Wang, et al. (1998). "Numb-associated kinase interacts with the phosphotyrosine binding domain of Numb and antagonizes the function of Numb in vivo." Mol Cell Biol **18**(1): 598-607.
- Conner, S. D. and S. L. Schmid (2002). "Identification of an adaptor-associated kinase, AAK1, as a regulator of clathrin-mediated endocytosis." J Cell Biol **156**(5): 921-9.
- Conner, S. D., T. Schroter, et al. (2003). "AAK1-mediated micro2 phosphorylation is stimulated by assembled clathrin." Traffic **4**(12): 885-90.
- Cooney, J. R., J. L. Hurlburt, et al. (2002). "Endosomal Compartments Serve Multiple Hippocampal Dendritic Spines from a Widespread Rather Than a Local Store of Recycling Membrane." J. Neurosci. **22**(6): 2215-2224.
- Corty, M. M., B. J. Matthews, et al. (2009). "Molecules and mechanisms of dendrite development in *Drosophila*." Development **136**(7): 1049-1061.

- de Renzis, S., B. Sonnichsen, et al. (2002). "Divalent Rab effectors regulate the sub-compartmental organization and sorting of early endosomes." Nat Cell Biol **4**(2): 124-33.
- Grueber, W. B., L. Y. Jan, et al. (2002). "Tiling of the Drosophila epidermis by multidendritic sensory neurons." Development **129**(12): 2867-2878.
- Hales, C. M., J. P. Vaerman, et al. (2002). "Rab11 family interacting protein 2 associates with Myosin Vb and regulates plasma membrane recycling." J Biol Chem **277**(52): 50415-21.
- Henderson, D. M. and S. D. Conner (2007). "A novel AAK1 splice variant functions at multiple steps of the endocytic pathway." Mol Biol Cell **18**(7): 2698-706.
- Horton, A. C. and M. D. Ehlers (2003). "Dual modes of endoplasmic reticulum-to-Golgi transport in dendrites revealed by live-cell imaging." Journal of Neuroscience **23**(15): 6188-6199.
- Horton, A. C., B. Racz, et al. (2005). "Polarized secretory trafficking directs cargo for asymmetric dendrite growth and morphogenesis." Neuron **48**(5): 757-771.
- Jordens, I., M. Fernandez-Borja, et al. (2001). "The Rab7 effector protein RILP controls lysosomal transport by inducing the recruitment of dynein-dynactin motors." Curr Biol **11**(21): 1680-5.
- Kennedy, M. J. and M. D. Ehlers (2006). "Organelles and trafficking machinery for postsynaptic plasticity." Annual Review of Neuroscience **29**: 325-362.
- Nakagawa, T., M. Setou, et al. (2000). "A novel motor, KIF13A, transports mannose-6-phosphate receptor to plasma membrane through direct interaction with AP-1 complex." Cell **103**(4): 569-81.
- Newpher, T. M. and M. D. Ehlers (2008). "Glutamate receptor dynamics in dendritic microdomains." Neuron **58**(4): 472-497.
- Nielsen, E., F. Severin, et al. (1999). "Rab5 regulates motility of early endosomes on

- microtubules." Nat Cell Biol **1**(6): 376-82.
- Park, M., E. C. Penick, et al. (2004). "Recycling endosomes supply AMPA receptors for LTP." Science **305**(5692): 1972-1975.
- Park, M., J. M. Salgado, et al. (2006). "Plasticity-Induced Growth of Dendritic Spines by Exocytic Trafficking from Recycling Endosomes." Neuron **52**(5): 817-830.
- Parrish, J. Z., K. Emoto, et al. (2007). "Mechanisms that regulate establishment, maintenance, and remodeling of dendritic fields." Annual Review of Neuroscience **30**: 399-423.
- Peng, Y. H., W. K. Yang, et al. (2009). "Nak regulates Dlg basal localization in *Drosophila* salivary gland cells." Biochem Biophys Res Commun **382**(1): 108-13.
- Satoh, D., D. Sato, et al. (2008). "Spatial control of branching within dendritic arbors by dynein-dependent transport of Rab5-endosomes." Nat Cell Biol **10**(10): 1164-71.
- Sholl, D. A. (1953). "Dendritic organization in the neurons of the visual and motor cortices of the cat." J Anat **87**(4): 387-406.
- Smythe, E. and K. R. Ayscough (2003). "The Ark1/Prk1 family of protein kinases. Regulators of endocytosis and the actin skeleton." EMBO Rep **4**(3): 246-51.
- Stone, M. C., F. Roegiers, et al. (2008). "Microtubules Have Opposite Orientation in Axons and Dendrites of *Drosophila* Neurons." Mol. Biol. Cell **19**(10): 4122-4129.
- Toshima, J., J. Y. Toshima, et al. (2005). "Phosphoregulation of Arp2/3-dependent actin assembly during receptor-mediated endocytosis." Nat Cell Biol **7**(3): 246-54.
- Wucherpfennig, T., M. Wilsch-Brauninger, et al. (2003). "Role of *Drosophila* Rab5 during endosomal trafficking at the synapse and evoked neurotransmitter release." J. Cell Biol. **161**(3): 609-624.
- Ye, B., Y. Zhang, et al. (2007). "Growing dendrites and axons differ in their reliance on

the secretory pathway." Cell **130**(4): 717-729.

Zheng, Y., J. Wildonger, et al. (2008). "Dynein is required for polarized dendritic transport and uniform microtubule orientation in axons." Nat Cell Biol **10**(10): 1172-80.



Figure 1. Distributions of endocytic markers in da dendrites.

(A, B) Rab4mRFP (white in A, green in B) was expressed in *109(2)80 > mCD8GFP* (red in B) neurons. Large puncta were observed at branch points (arrowheads), small puncta were observed in dendritic shafts (arrows)

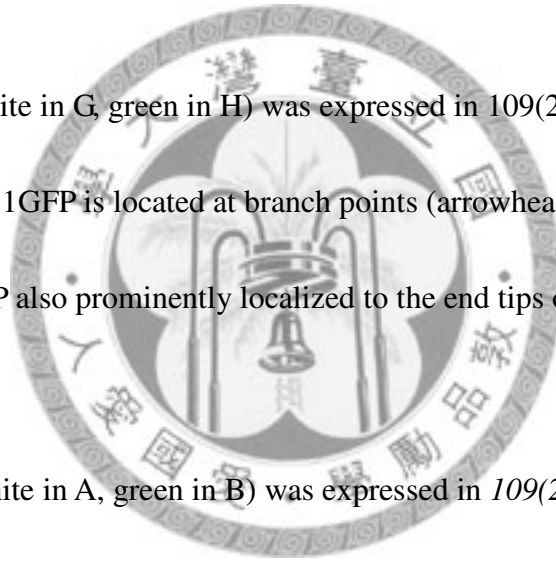
(C, D) Rab5GFP (white in C, green in D) was expressed in *109(2)80 > myrmRFP* (red in D) neurons. Rab5GFP is also located at branch points (arrowheads) and dendritic shafts (arrows).

(E, F) Rab11GFP (white in E, green in F) was expressed in *109(2)80 > myrmRFP* (red in F) neurons. Rab11GFP is located at branch points (arrowheads) and dendritic shafts (arrows). Rab11GFP also prominently localized to the end tips of dendritic processes (asterisks).

(G, H) ManIIIGFP (white in G, green in H) was expressed in *109(2)80 > myrmRFP* (red in H) neurons. Branch point-localizing signals (arrowheads), and dendritic shafts localizing puncta (arrows) were indicated.

(I, J) YFPNak (white in I, green in J) was expressed in *109(2)80 > myrmRFP* (red in J) neurons, and was branch-points (arrowheads) and dendritically (arrows) localized. Sometimes we can observe large patches of YFPNak in the shafts (asterisks).

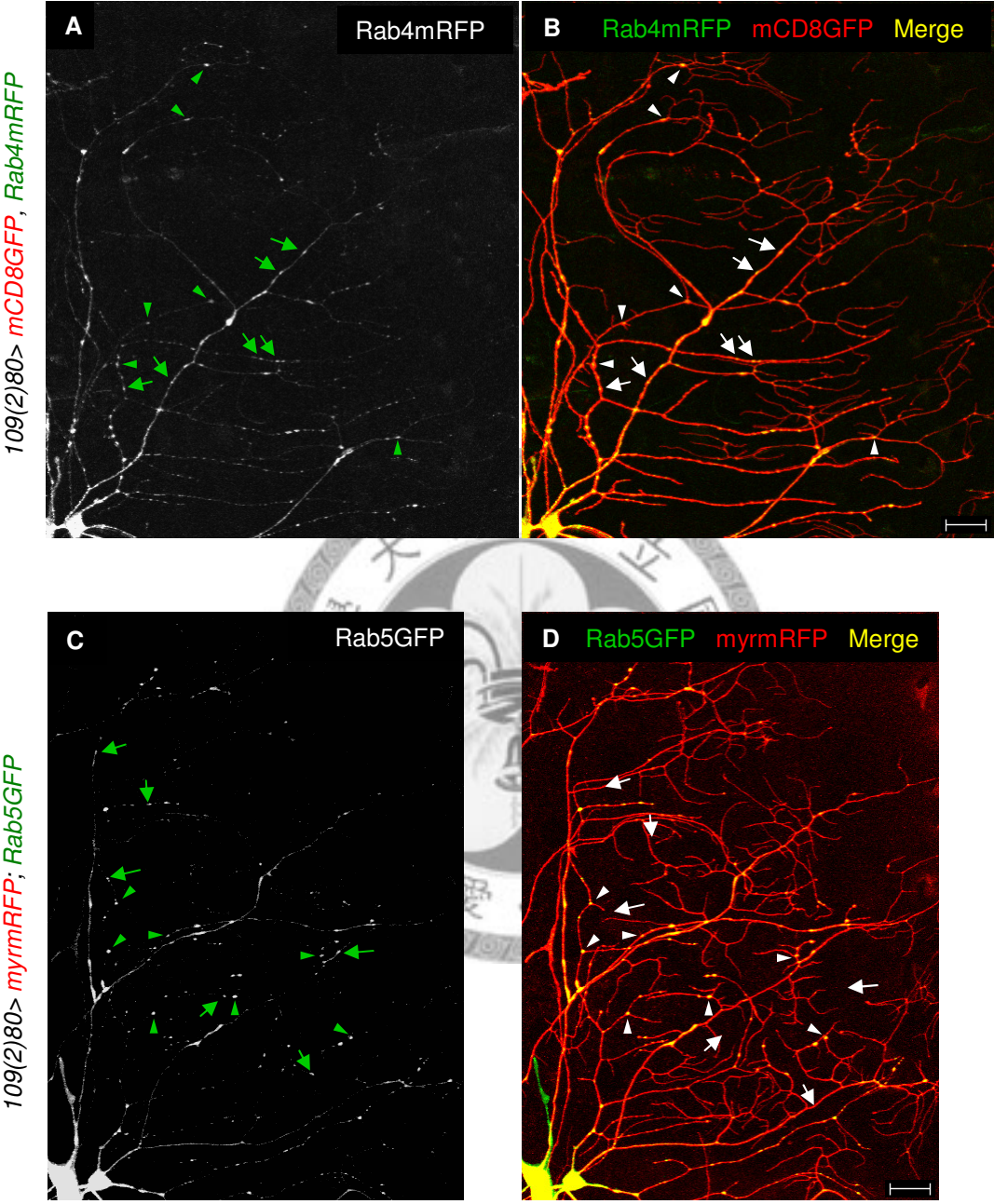
(K-O) Straighten dendrites from (A-J). Dendrites were marked by either *mCD8GFP* (K, red) or *myrmRFP* (L-O, red). The markers were shown in monochrome as well as



merged image with dendrites. (K) Rab4mRFP puncta appeared the most at proximal dendrites and decreased as the distance from soma increased. (L) Rab5GFP distributed evenly along the process. (M) Rab11 can travel along the dendrites to reach the most distal part. (N) ManIIIGFP was evenly distributed. (O) YFPNak was equally distributed in the dendrites.



Figure. 1



Scale Bar = 20 μ m

Figure. 1 (cont.)

Scale Bar = 20 μ m

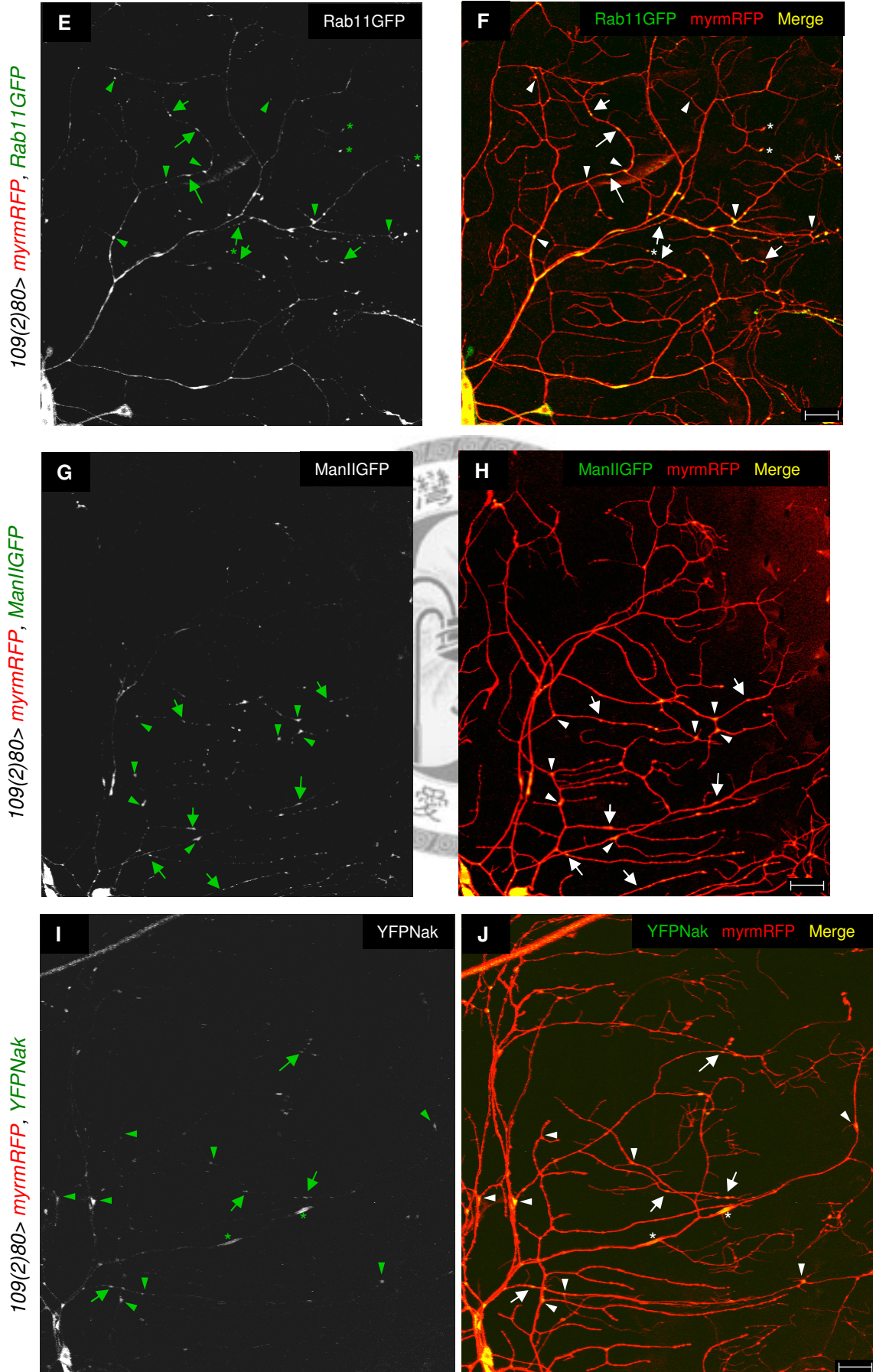


Figure. 1 (cont.)



Figure 2. Scoring results of the marker distributions.

(A) Simplified diagram to describe the scoring method. (B) Puncta numbers of Rab4mRFP, Rab5GFP, Rab11GFP, ManIIGFP, and YFPNak in each concentric interval were shown. Rab4mRFP was peaked at the region 150-175 μ m from soma, Rab5GFP peaked at region 175-200 μ m, and Rab11GFP at 200-225 μ m. (C) Distribution density indicators, Puncta number/ Dendrite, were plotted to their distances from soma.

Rab4mRFP displayed strong proximal distribution, Rab11GFP showed distal preference, and the others distributed equally. (D) Total puncta number/neuron was the highest in Rab4mRFP, the least in ManIIGFP and YFPNak. (E) Expression of markers did not exert dramatic differences in the dendrite numbers.

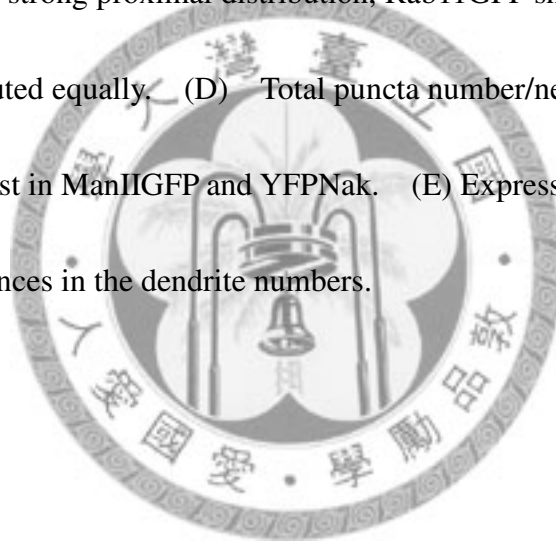
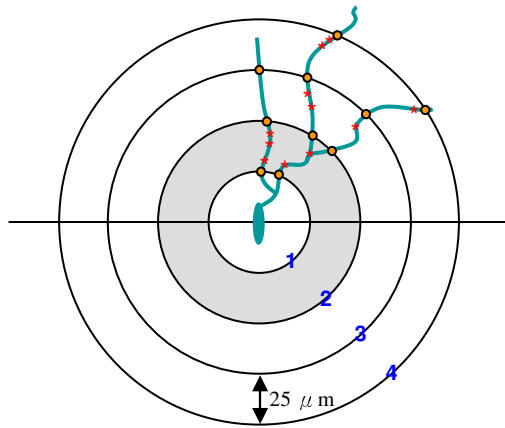


Figure. 2

A



- Cross-Over
- * Puncta

EX:
To score the region of 25-50 μm from the cell body
= score the upper hemisphere of shadowed region

Puncta No. = 5

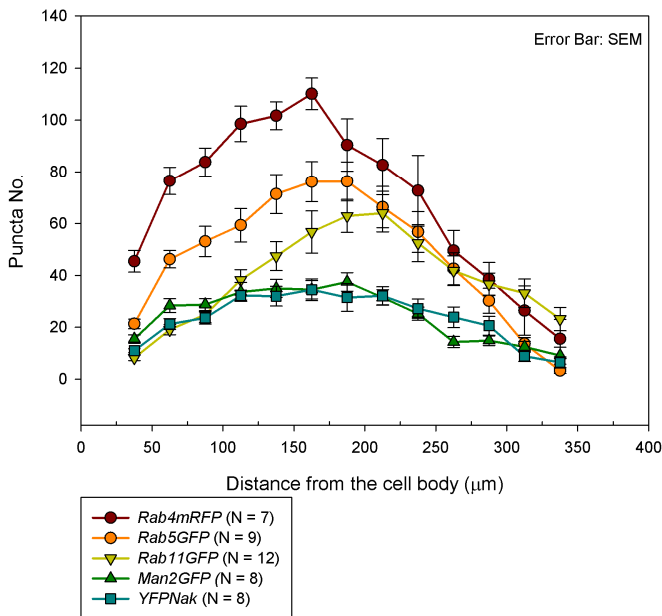
Dendrite No. = $(2 + 3) / 2 = 2.5$

Intersections (Circle 1) = 2

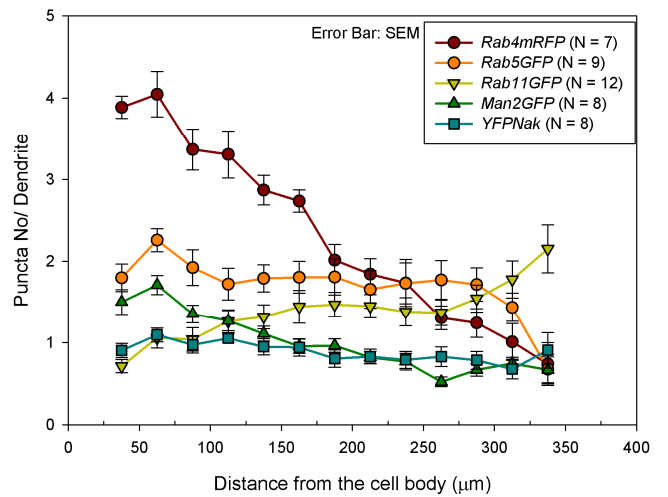
Intersections (Circle 2) = 3

Puncta No./ Dendrite = $5 / 2.5 = 2$

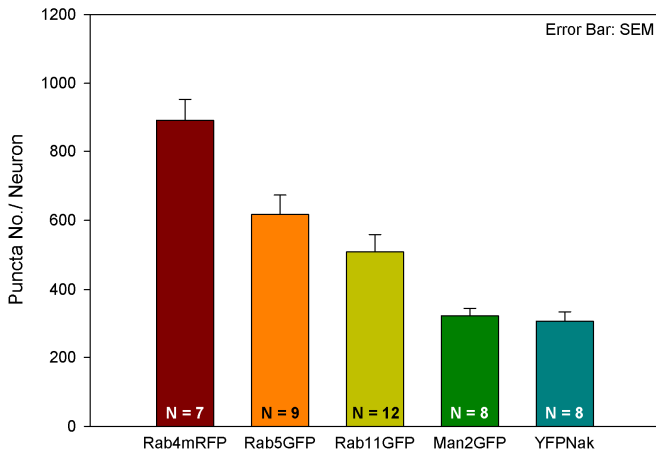
B



C



D



E

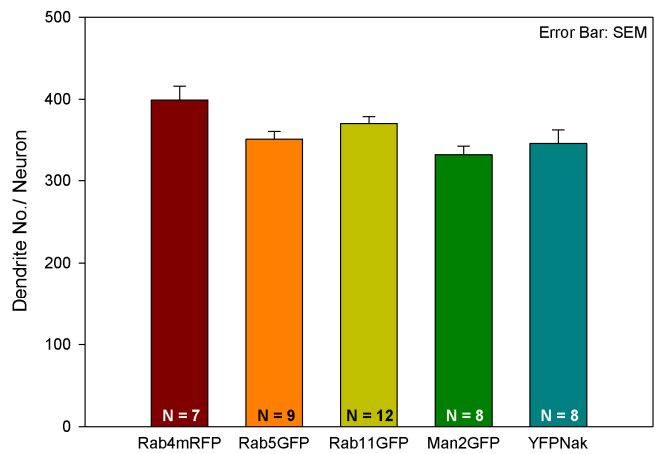


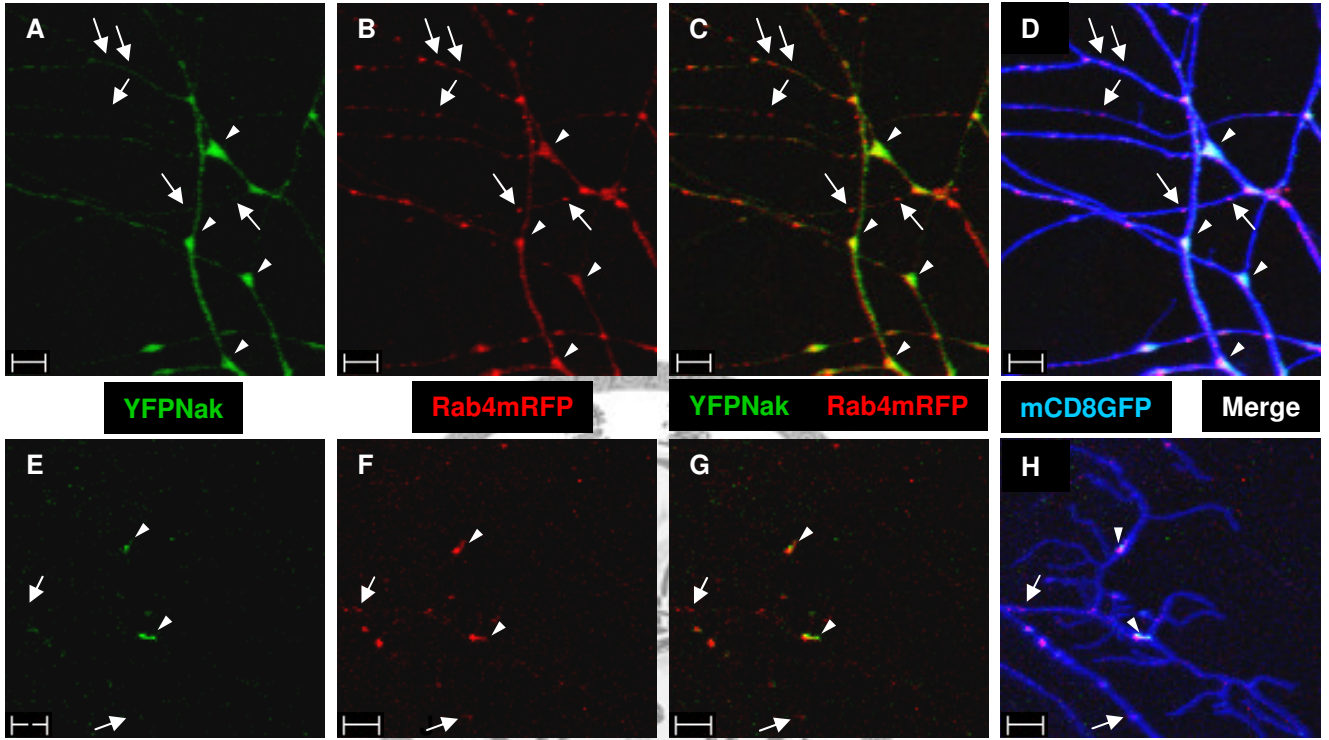
Figure 3. Rab4mRFP partially colocalized with YFPNak

Rab4mRFP and YFPNak were coexpressed in $109(2)80 > mCD8GFP$ neurons. Good colocalizations at branch points in proximal (A-D, arrowheads) and distal (E-H, arrowheads) branches were observed. Note that within the colocalized puncta, YFPNak signals were usually with larger areas than Rab4mRFP. Moreover, there were also small Rab4mRFP puncta in the dendritic shafts which did not colocalized with YFPNak (A-H, arrows).



Figure. 3

109(2)80> *mCD8GFP, Rab4mRFP; YFPNak*



Scale Bar = 10 μ m

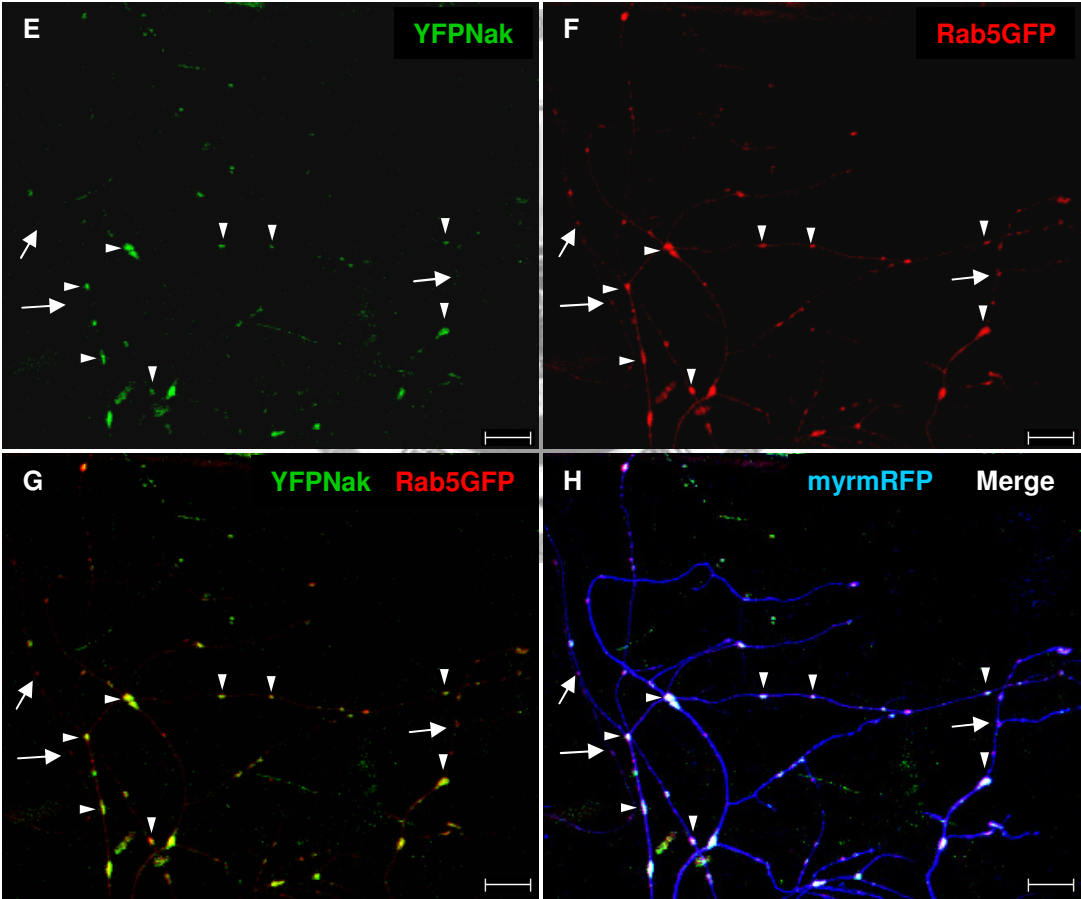
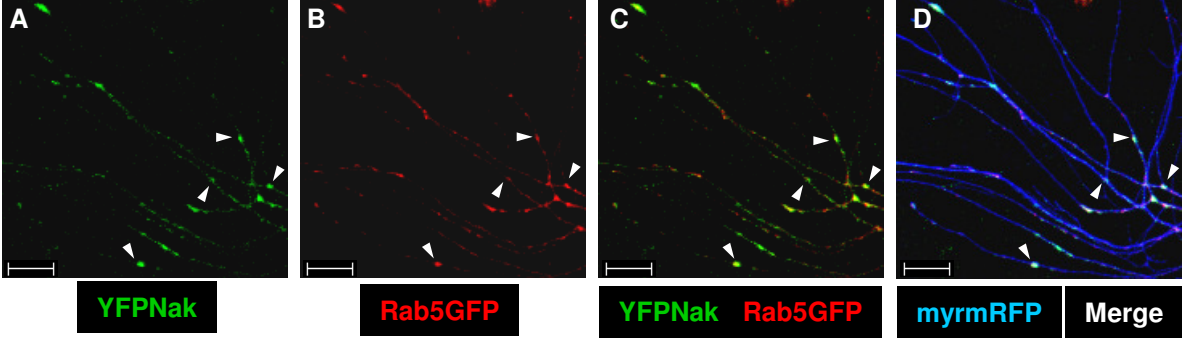
Figure 4. Rab5GFP partially colocalized with YFPNak

Rab5GFP and YFPNak were coexpressed in *109(2)80 > myrmRFP* neurons. Good colocalizations at branch points as well as dendritic processes in proximal (A-D, arrowheads) and distal (E-H, arrowheads) branches were observed. However, there were still some YFPNak and Rab5GFP signals not overlapped (A-H, arrows), which located primarily in dendritic shafts.



Figure. 4

109(2)80> *myrmRFP*; *YFPNak*, *Rab5GFP*



Scale Bar = 20 μ m

Figure 5. Rab11GFP partially colocalized with YFPNak

Rab11GFP and YFPNak were coexpressed in *109(2)80 > myrmRFP* neurons. Good colocalizations at branch points as well as dendritic processes in proximal (A-D, arrowheads) and distal (E-H, arrowheads) branches were observed. There were also not overlapping YFPNak and Rab11GFP signals (A-H, arrows).



Figure. 5

109(2)80> *myrmRFP*, *Rab11GFP*; *YFPNak*

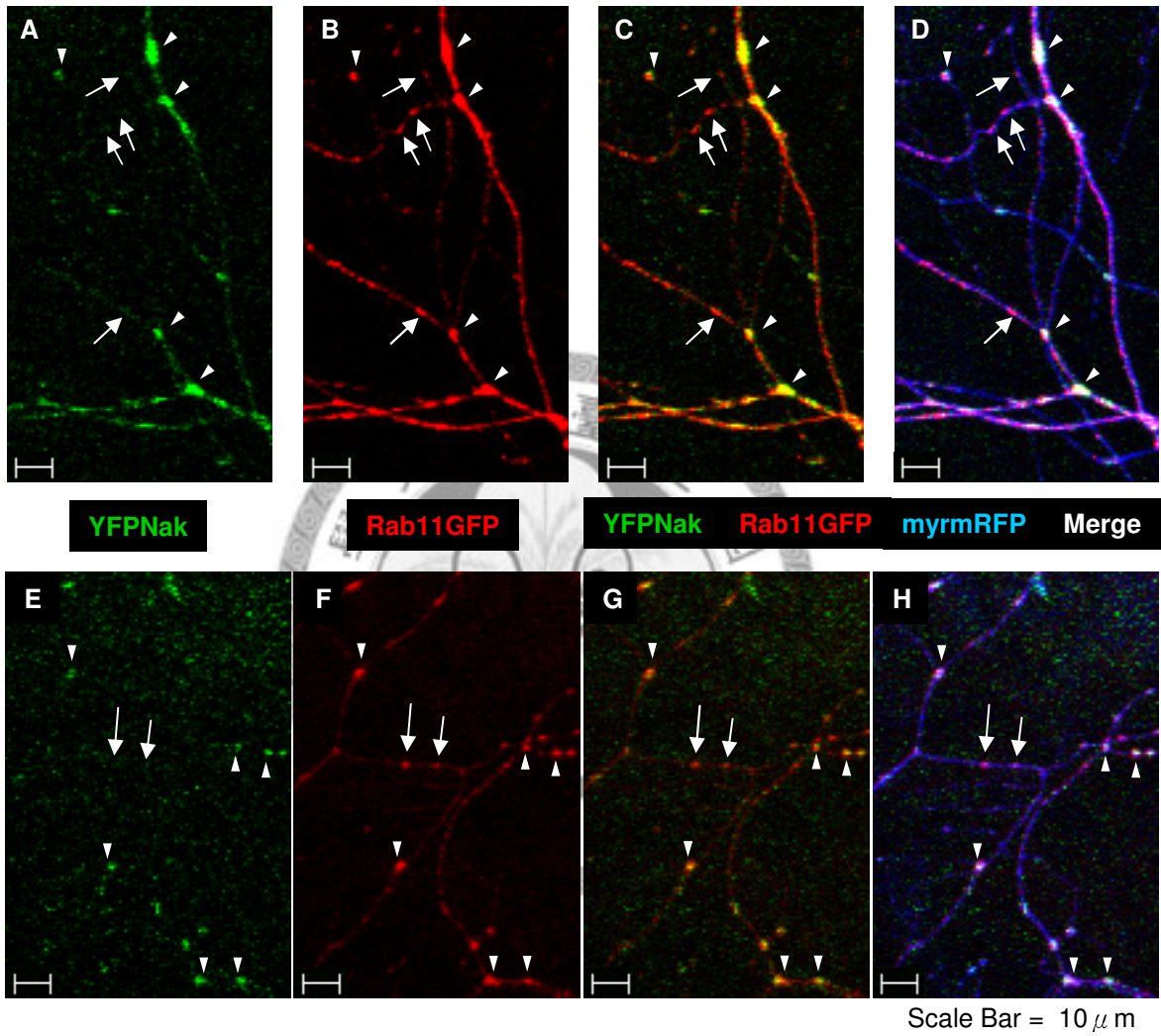


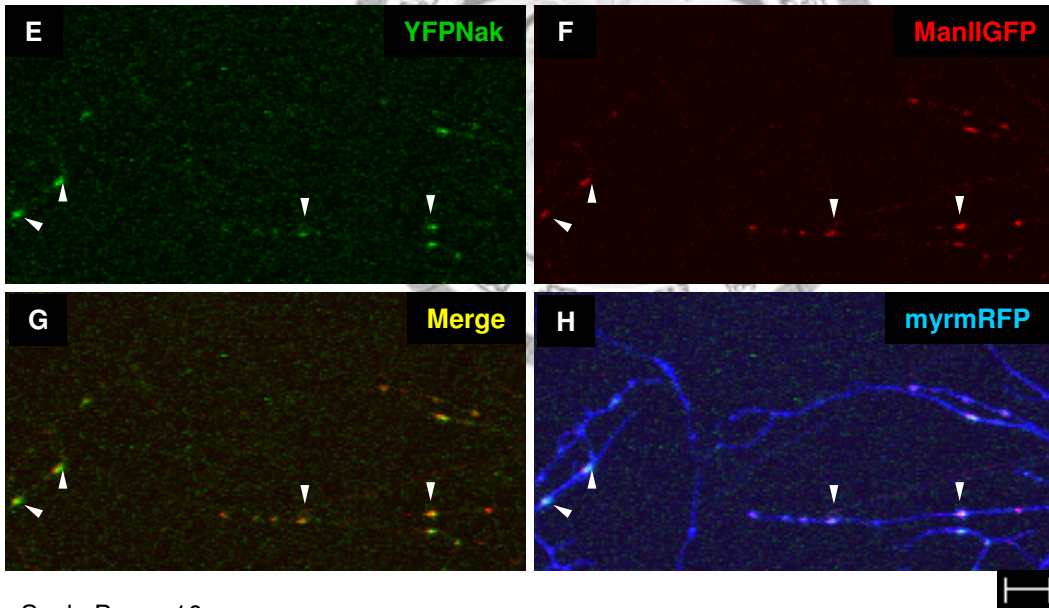
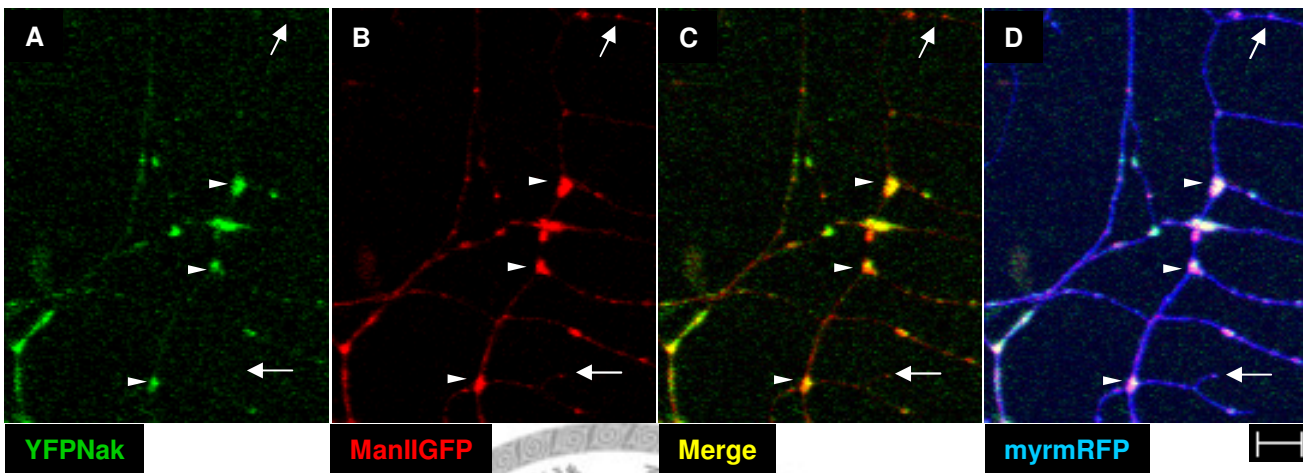
Figure 6. ManIIGFP partially colocalized with YFPNak

ManIIGFP and YFPNak were coexpressed in *109(2)80 > myrmRFP* neurons. They showed good colocalization in proximal (A-D, arrowheads) and distal (E-H, arrowheads) dendrites.



Figure. 6

109(2)80> *myrmRFP*, *ManII*GFP; *YFP*Nak



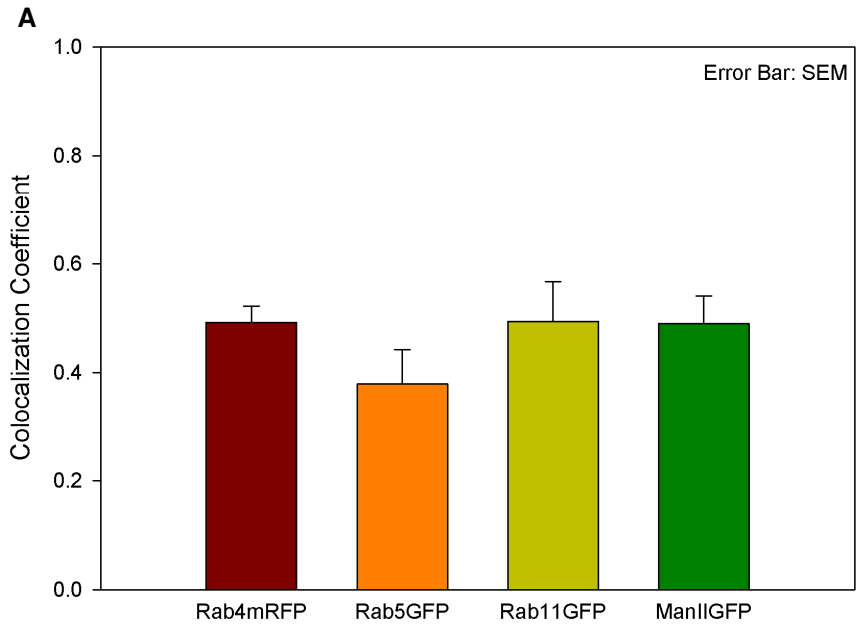
Scale Bar = 10 μ m

Figure 7. Colocalization status between YFPNak and endocytic compartments

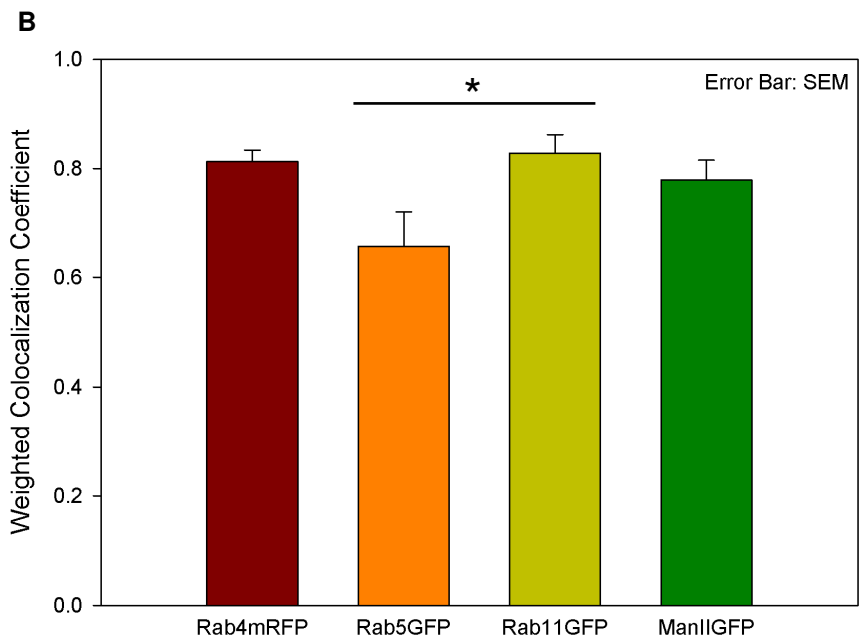
The scoring results of Fig. 3-6 demonstrating the colocalization coefficients (A) and weighted colocalization coefficients (B) of YFPNak and endocytic markers. Deep red bars: Rab4mRFP, Orange bars: Rab5GFP, Yellow bars: Rab11GFP, Green bars: ManIIIGFP.



Figure. 7



Colocalization Coefficient
= Colocalized YFP pixel number / Total YFP pixel number



Weighted Colocalization Coefficient
= Colocalized YFP Intensity / Total YFP intensity

Figure 8. ClcGFP distribution was dramatically influenced by *nak* RNAi

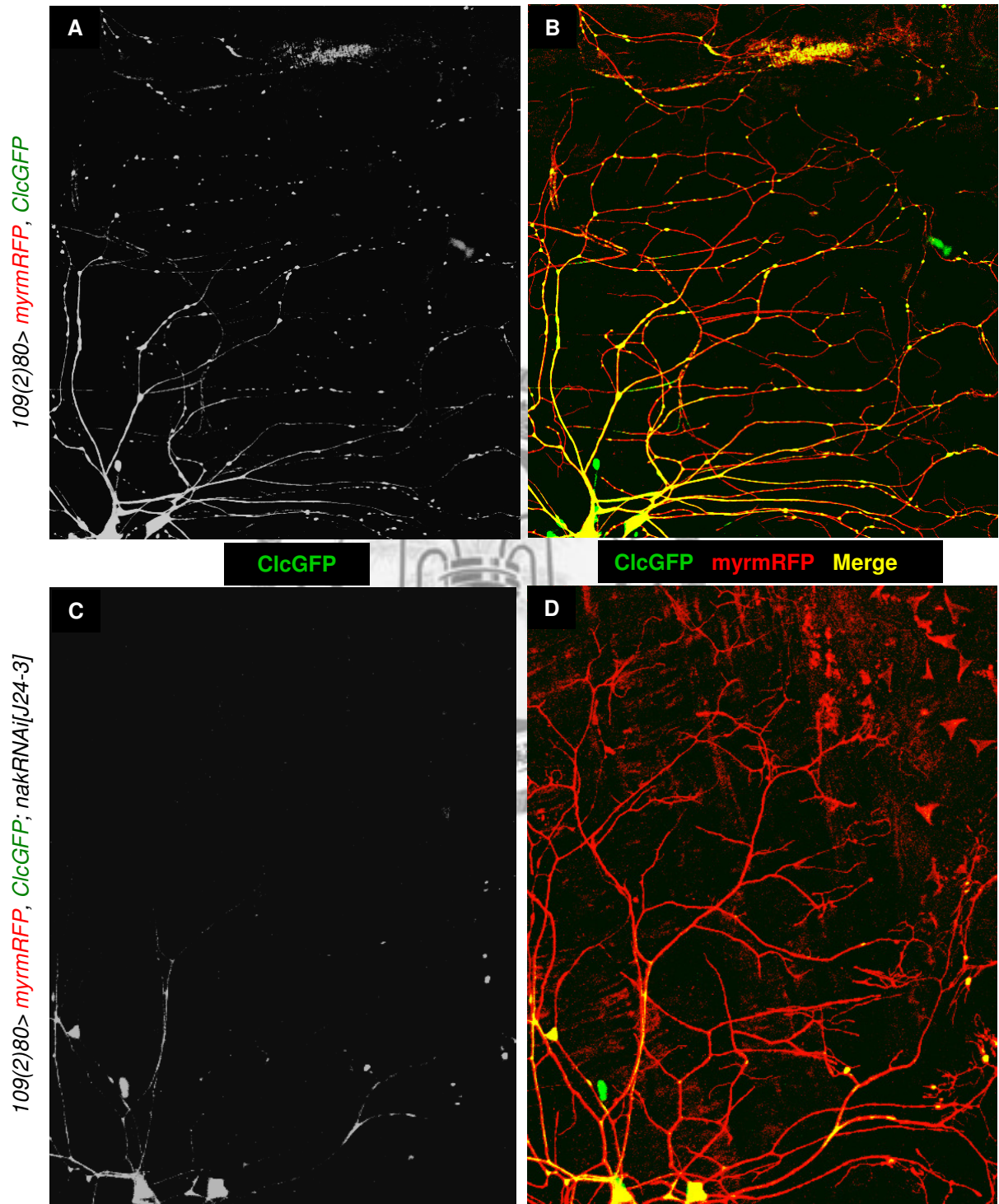
109(2)80 > myrmRFP, ClcGFP neurons with (C and D) or without *nak* RNAi

coexpression (A and B) are shown. ClcGFP puncta were shown in green (A-D) and dendrite morphologies were labeled with *109(2)80>myrmRFP* (red in B and D). The ClcGFP puncta in *nak* RNAi expressing neurons (C-D) was reduced dramatically.

(Images were obtained by Wei-Kan Yang)



Figure. 8



(By Wei-Kan Yang, unpublished)

Figure 9. *nak* depletion globally reduced the puncta number along the dendrites

This is the statistic results of ClcGFP in control (*109(2)80Gal4*) and *nak* knockdown da dendrites. (A) ClcGFP puncta numbers were plotted against their distance from the cell body. Significant reduction of puncta numbers was observed. (B) Dendrite numbers were plotted to the distance from soma, and a significant dendritic loss was observed in *nak* RNAi expression neurons. (C) The densities of ClcGFP were plotted to their distance from soma, the distributions of ClcGFP densities were dramatically reduced by *nak* RNAi expression. (D) The puncta number and dendrite number of each neuron were summed. The puncta number/neuron showed striking decrease and the dendrite number/ neuron was also significantly reduced in *nak* depleted neurons.

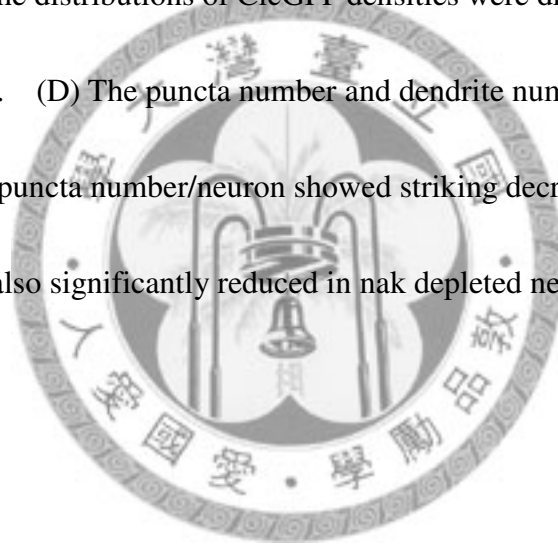


Figure. 9

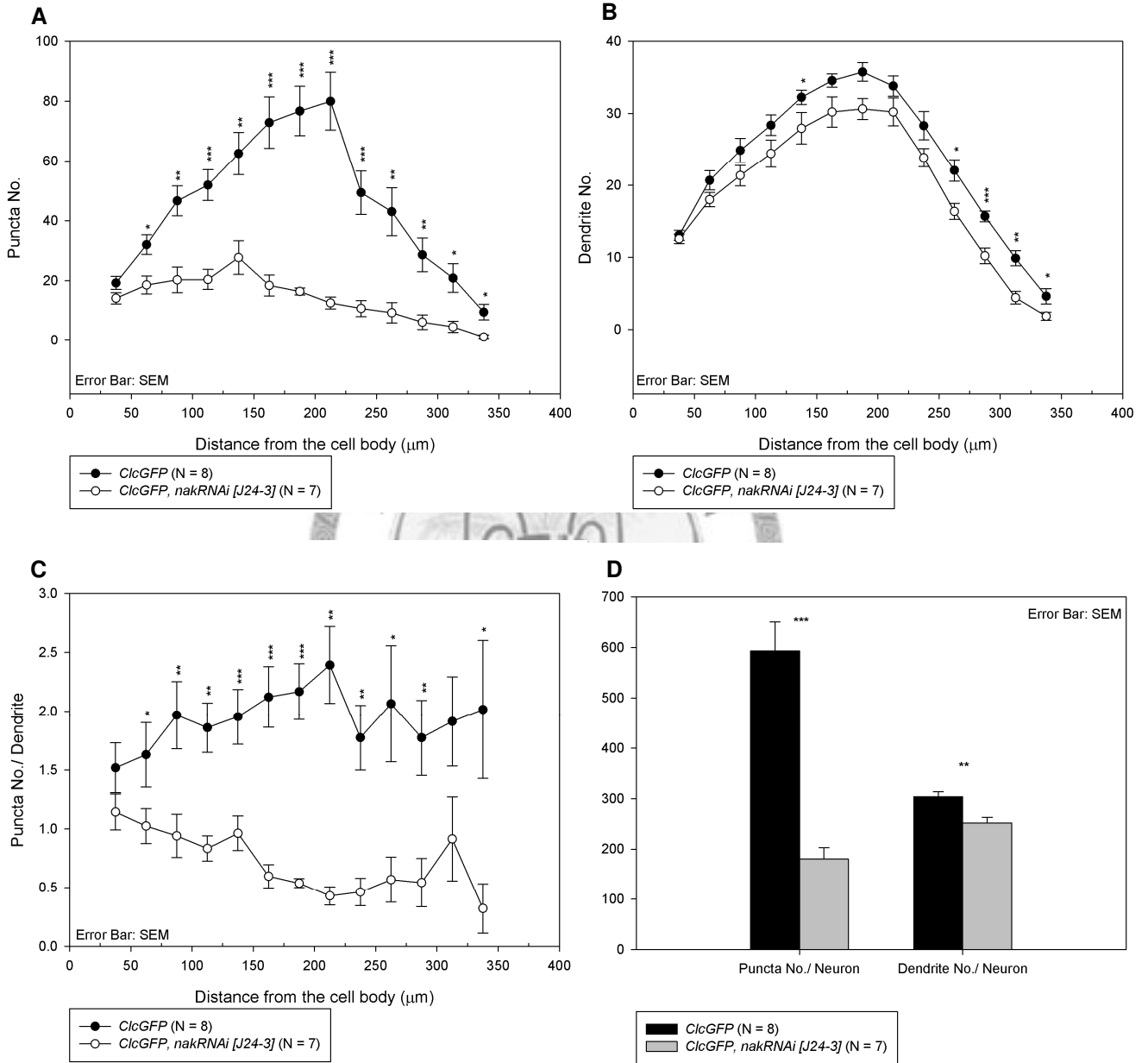


Figure 10. Rab4mRFP distribution in dendrites was not altered by nak depletion

109(2)80 > mCD8GFP, Rab4mRFP neurons were coexpressed with either lacZ (A and B) or *nak* RNAi (C and D). Rab4mRFP puncta were shown in green (B and D) and dendrite morphologies were labeled with *109(2)80>mCD8GFP* (red in B and D). Single channel images of Rab4mRFP were shown in A and C. The dendritic distribution pattern of Rab4mRFP in *nak* RNAi expressing neurons (C-D) is similar to lacZ control neurons (A-B). Scale bar = 20 μ m.



Figure. 10

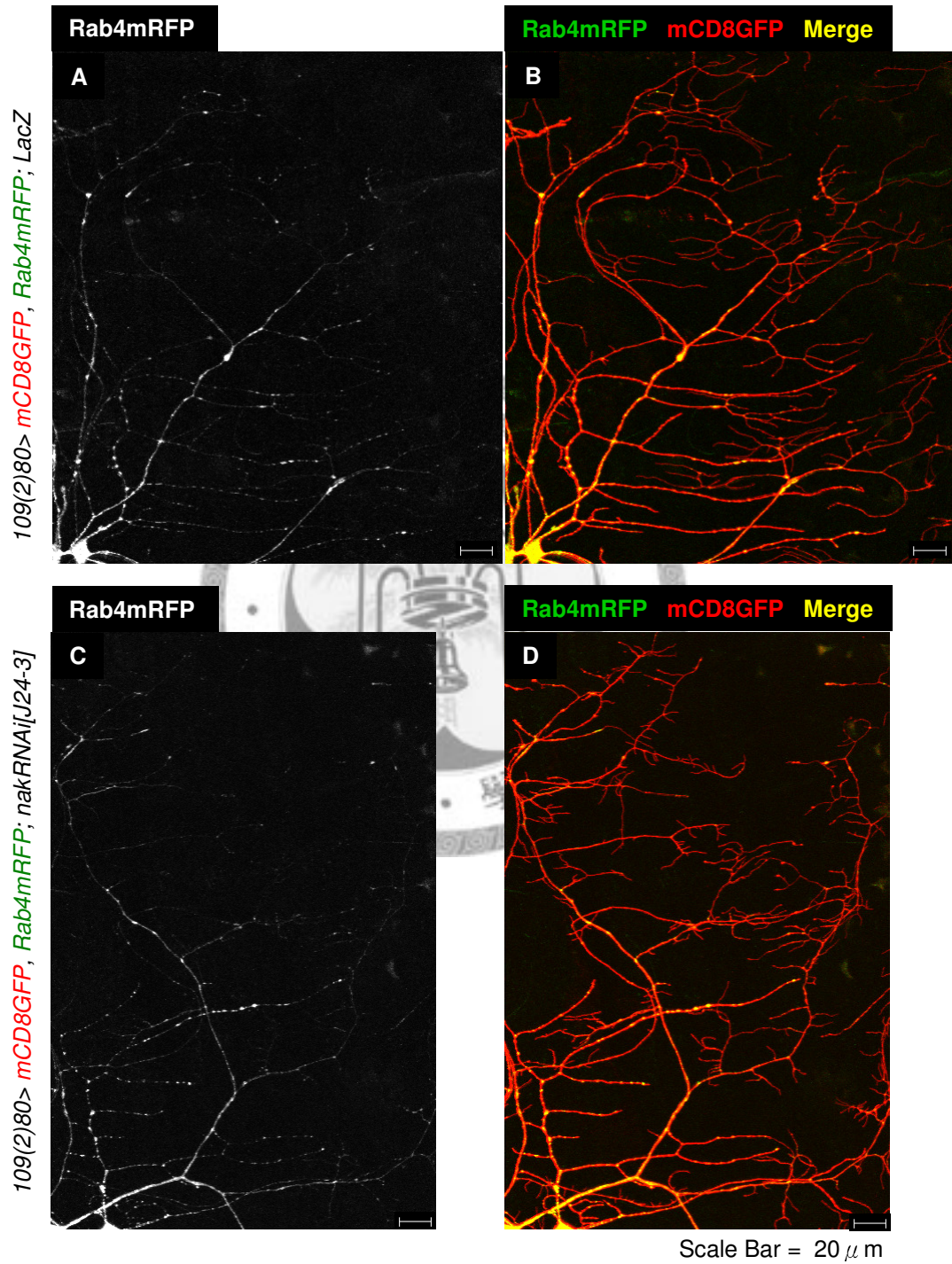


Figure 11. Rab4mRFP puncta number and distribution was not sensitive to Nak level

This is the statistics results of Rab4mRFP in control and *nak* knockdown da dendrites.

(A) Puncta numbers of Rab4mRFP puncta distribution along the dendrites showed no difference between control and Nak knockdown dendrites. (B) However, *nak* RNAi expression did not exert strong dendritic phenotype, either. (C) The distributions of Rab4mRFP were not affected by *nak* RNAi expression. (D) Puncta number and dendrite number were not changed by *nak* RNAi.



Figure. 11

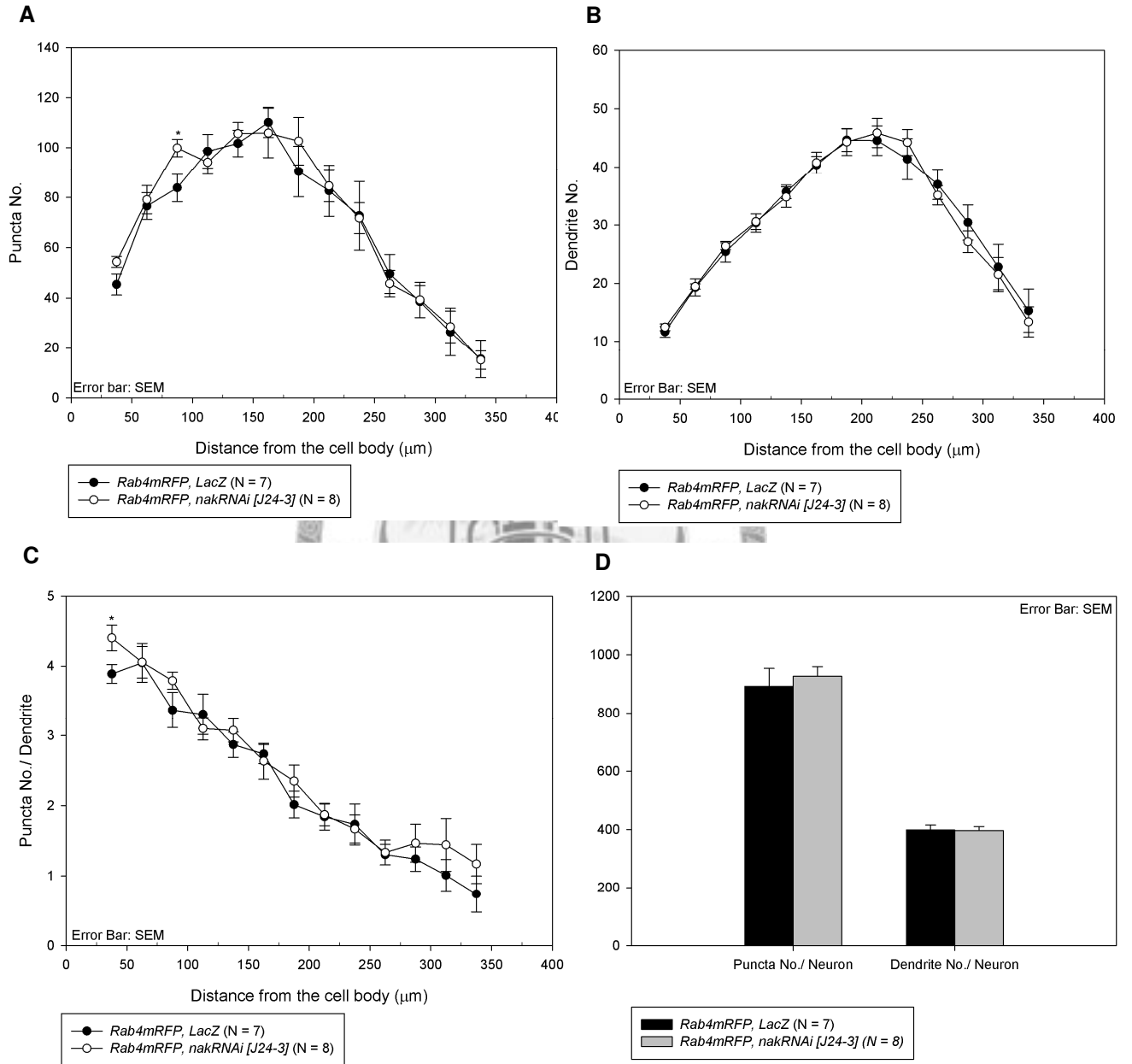


Figure 12. Rab5GFP distribution in dendrites was not altered by nak depletion

Either lacZ (A-B) or *nak* RNAi (C-D) were expressed in *109(2)80 > myrmRFP*, *Rab5GFP* neurons. Rab5GFP puncta were shown in green (B and D) and the myrmRFP-marked dendritic morphologies were shown in red (B and D). Single channel images of Rab5GFP were shown (A and C). The dendritic distribution pattern of Rab5GFP in control neurons (A-B) was similar in *nak* RNAi expressing dendrites (C-D). Scale bar = 20 μ m.



Figure. 12

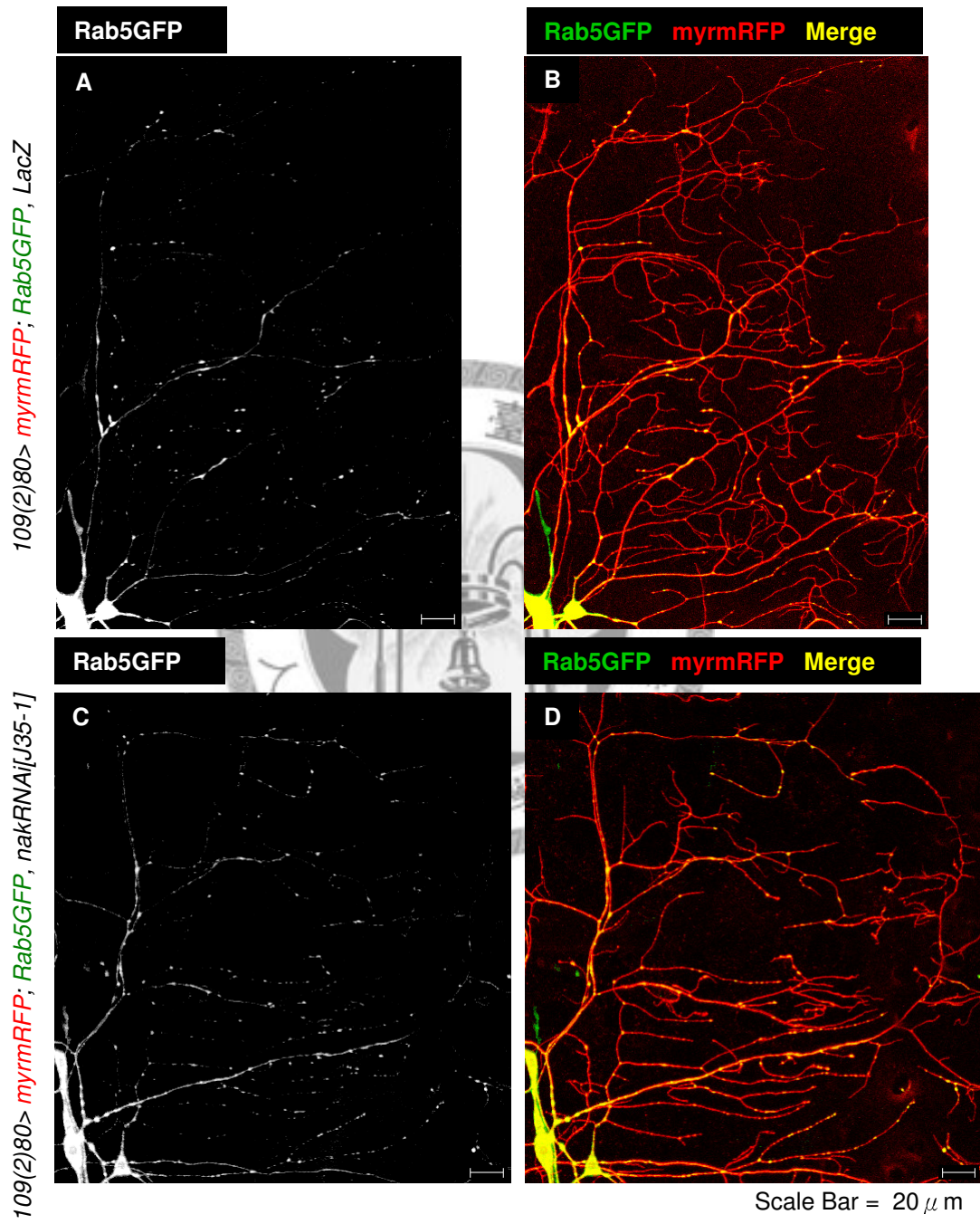


Figure 13. Rab5GFP puncta number and distribution was not sensitive to Nak level

This is the statistic results of Rab5GFP in control and *nak* knockdown da dendrites. (A)

Rab5GFP puncta numbers were plotted against the distance from the cell body. Their

distribution along the dendrites showed no difference between control and Nak

knockdown dendrites. (B) Dendrite numbers were plotted to the distance from soma,

and *nak* RNAi expression showed mild dendritic loss. (C) The densities of Rab5GFP

were plotted to their distance from soma, the density distributions of Rab5GFP were not

affected by *nak* RNAi expression. (D) The puncta number and dendrite number of

each neuron were summed. Dendrite number/ neuron was slightly decreased in *nak*

RNAi-expressing neurons, whereas the puncta number/neuron was unaltered.

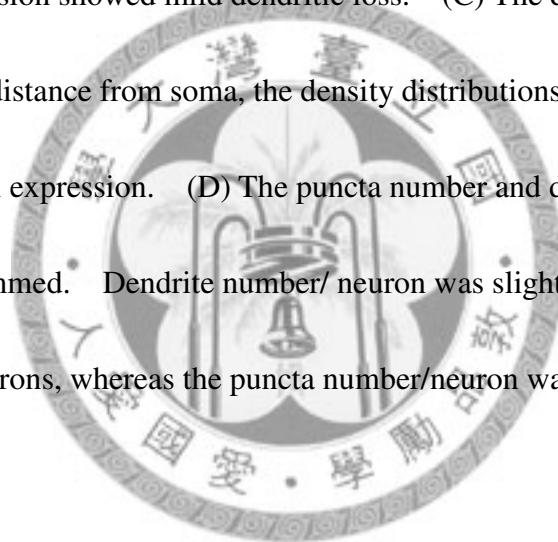


Figure. 13

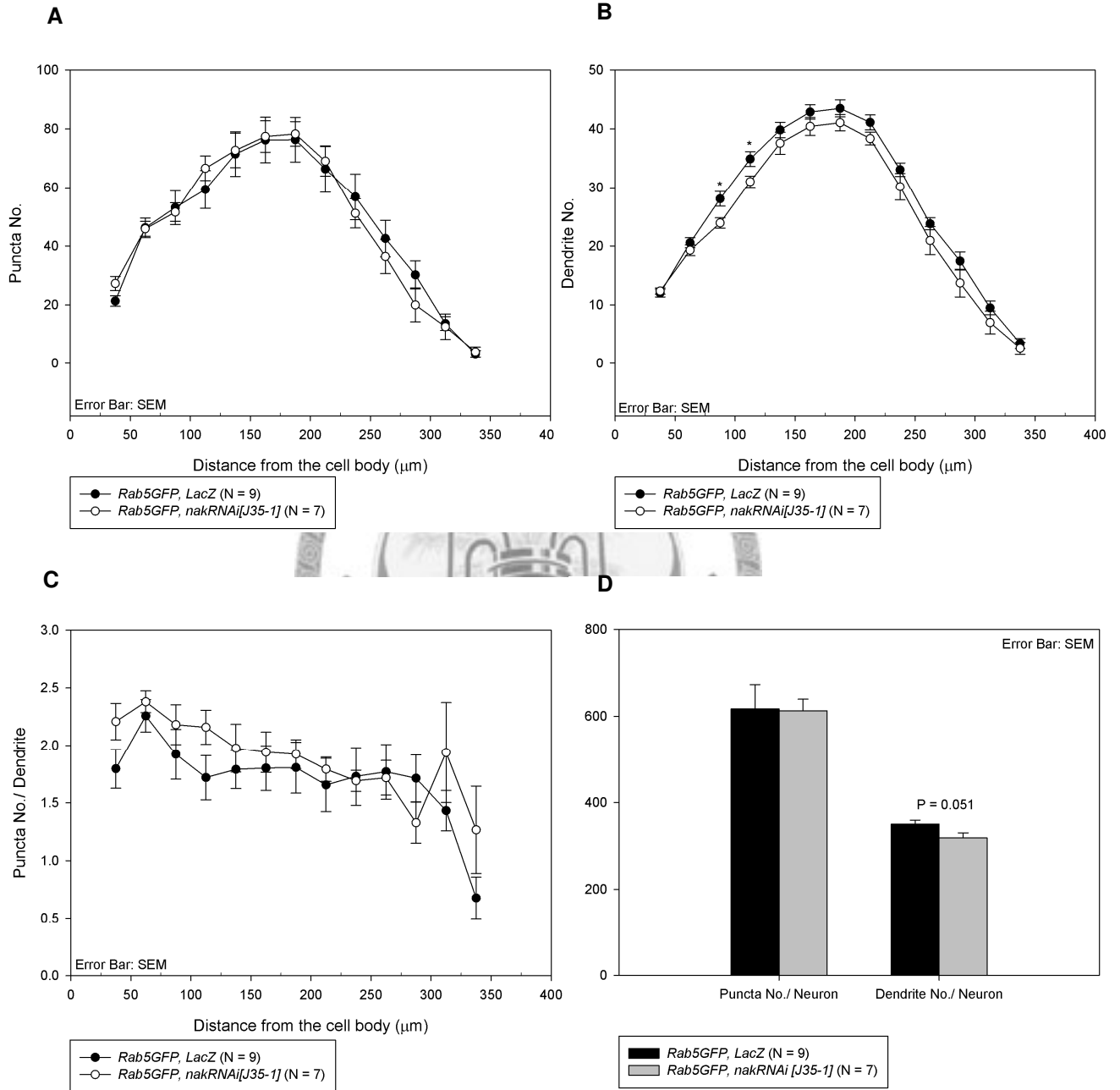


Figure 14. *nak* depletion did not affect Rab11GFP puncta number and distribution in dendrites

109(2)80 > myrmRFP, Rab11GFP neurons were coexpressed with either lacZ (A and B) or *nak* RNAi (C and D). Single channel images of Rab11GFP were shown in A and C. Rab11GFP puncta were shown in green (B and D) and dendrite morphologies were labeled with myrmRFP (red in B and D). The dendritic distribution pattern of Rab11GFP in *nak* RNAi expressing neurons (C-D) is similar to lacZ control neurons (A-B). Scale bar = 20 μ m.

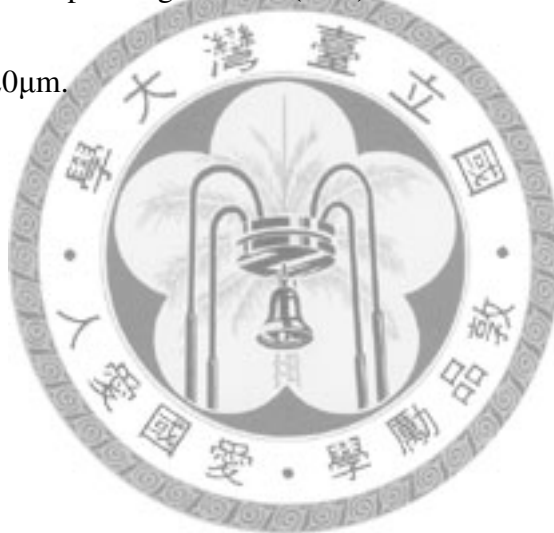


Figure. 14

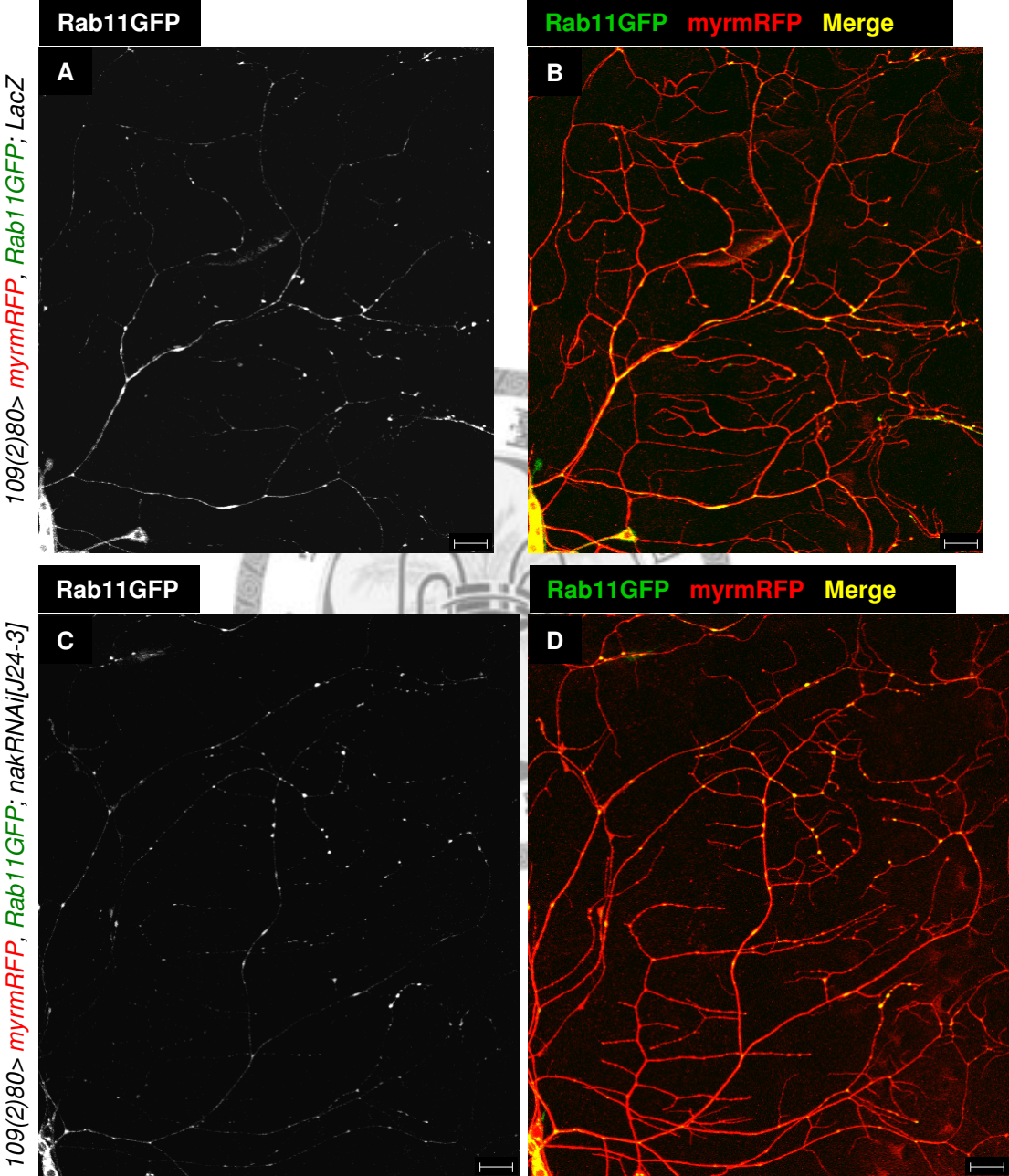


Figure 15. The number and distribution of Rab11GFP puncta was not affected in *nak* depleted neurons

This is the statistic results of Rab11GFP in lacZ control and *nak* knockdown da dendrites. (A) Rab11GFP puncta numbers were plotted against the distance from the cell body. Their distribution along the dendrites showed no significant differences between control and *Nak* knockdown dendrites. (B) Dendrite number were plotted to the distance from soma, and a mild but significant dendritic loss was observed in *nak* RNAi expressing neurons. (C) The densities of Rab11GFP were plotted to their distance from soma, the density distributions of Rab11GFP were not affected by *nak* RNAi expression. (D) The puncta number and dendrite number of each neuron were summed. The dendrite number/ neuron was reduced in *nak* depleted neurons and the puncta number/ neuron was unaltered.

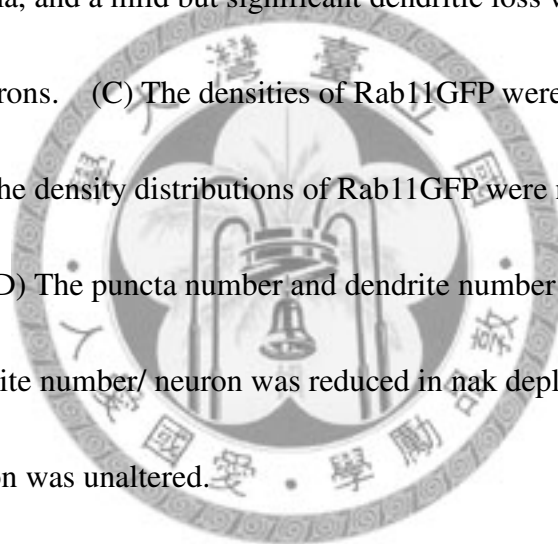


Figure. 15

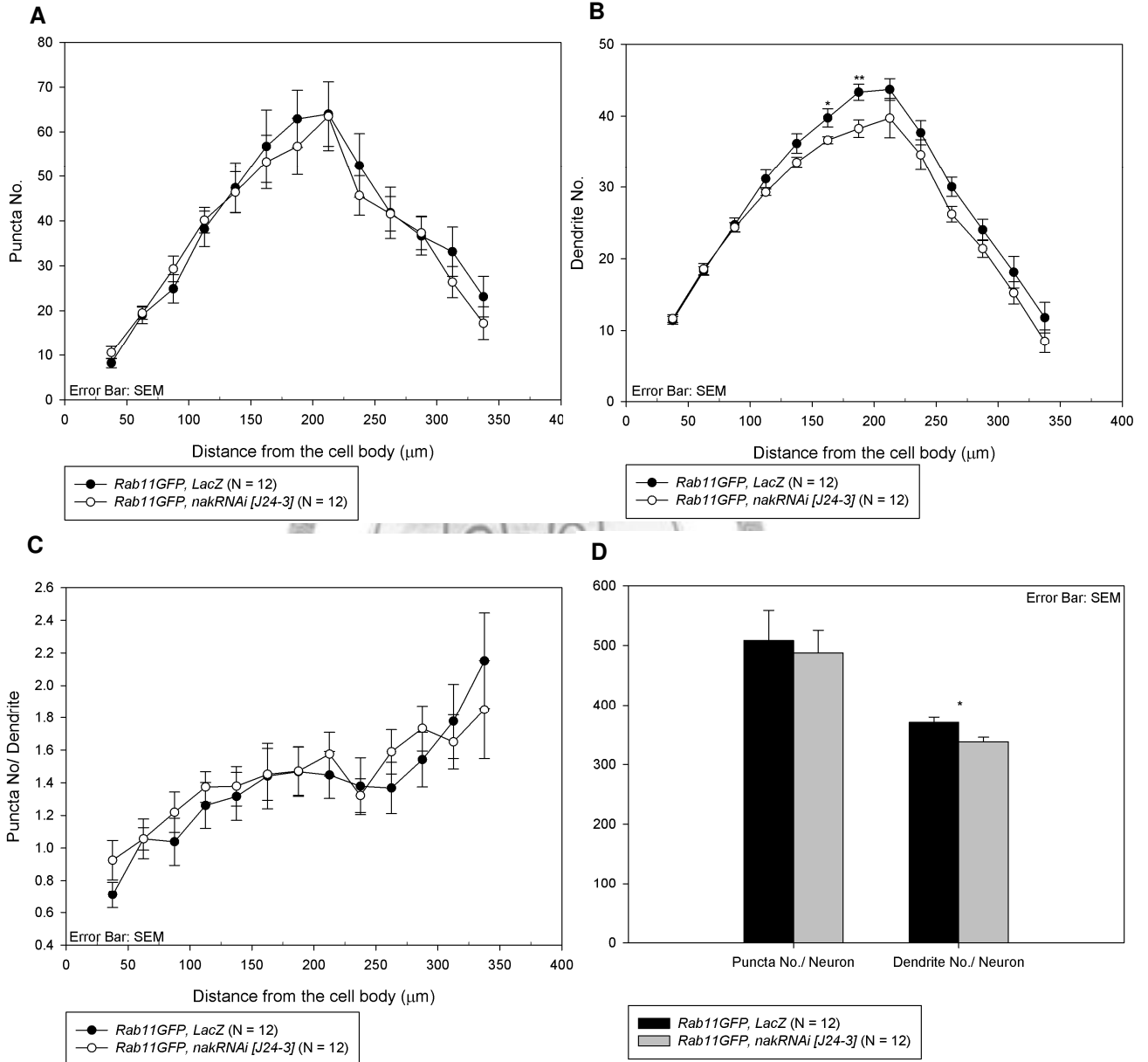


Figure 16. ManIIGFP distribution in dendrites was not altered by nak depletion

109(2)80 > myrmRFP, ManIIGFP neurons were coexpressed with either lacZ (A and B)

or *nak* RNAi (C and D). Single channel images of ManIIGFP were shown in A and C.

ManIIGFP puncta were shown in green (B and D) and dendrite morphologies were

labeled with *myrmRFP* (red in B and D). The dendritic distribution pattern of

ManIIGFP in *nak* RNAi expressing neurons (C-D) is similar to lacZ control neurons

(A-B). Scale bar = 20 μ m.



Figure. 16

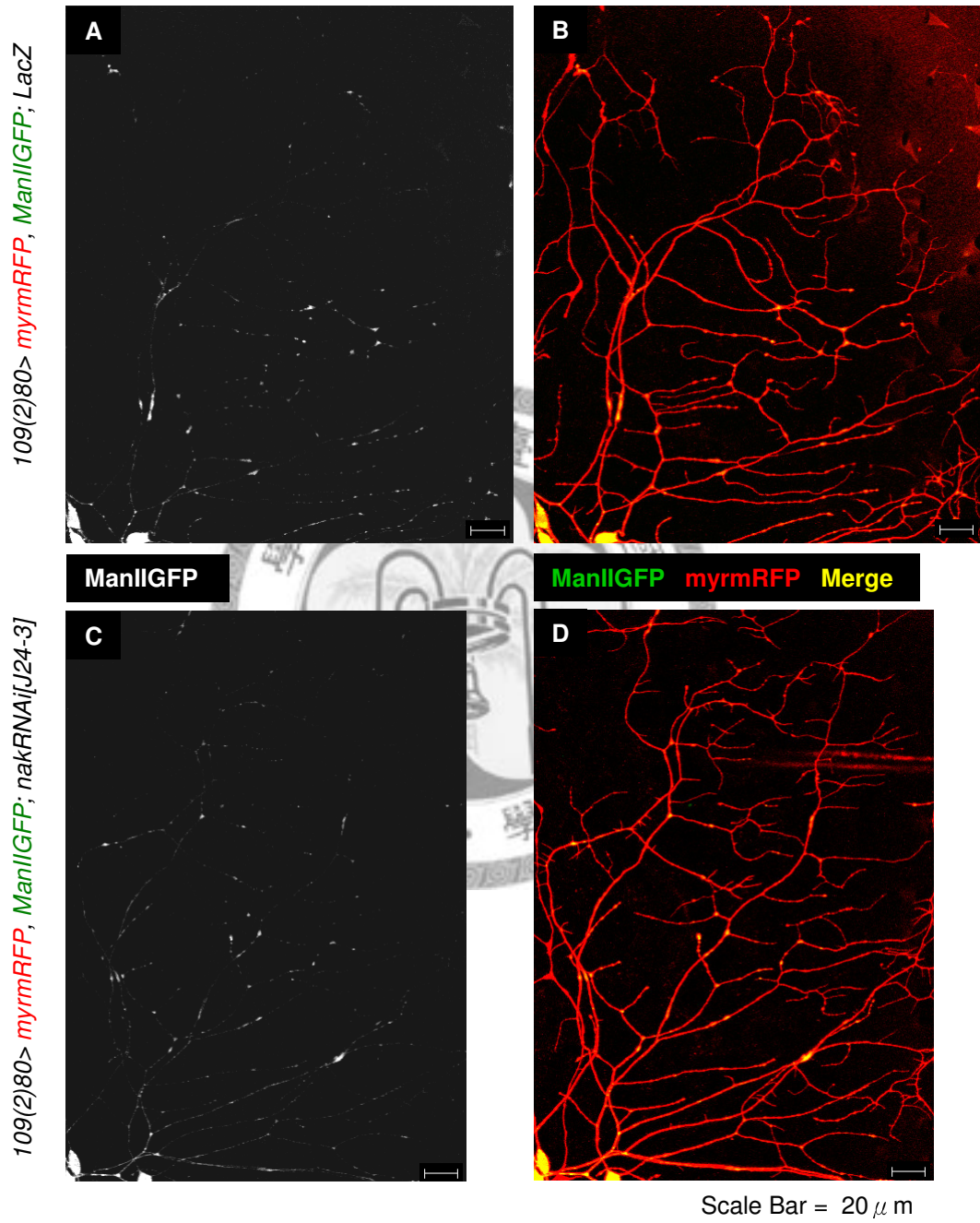


Figure 17. The number and distribution of ManIIIGFP puncta was not affected by *nak* RNAi expression

This is the statistic results of ManIIIGFP in lacZ control and *nak* knockdown da dendrites. (A) ManIIIGFP puncta numbers were plotted against the distance from the cell body. Their distribution along the dendrites showed no significant differences between control and *Nak* knockdown dendrites. (B) Dendrite number were plotted to the distance from soma, and mild dendritic loss was observed in *nak* RNAi expression neurons. (C) The densities of ManIIIGFP were plotted to their distance from soma, the density distributions of ManIIIGFP were not affected by *nak* RNAi expression. (D) The puncta number and branch index of each neuron were summed. Dendrite number/neuron and the puncta number/neuron were unaltered.

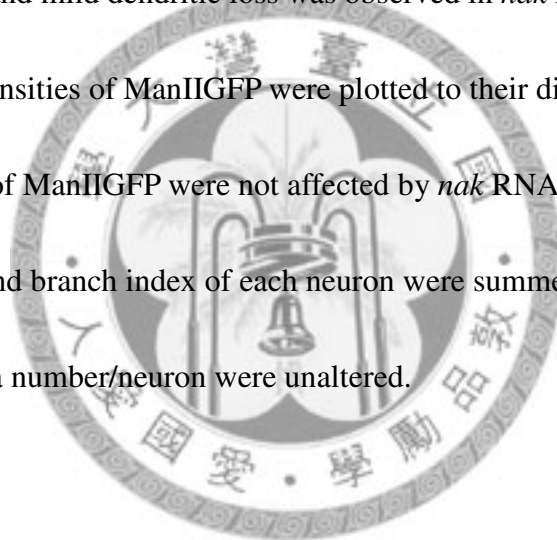


Figure. 17

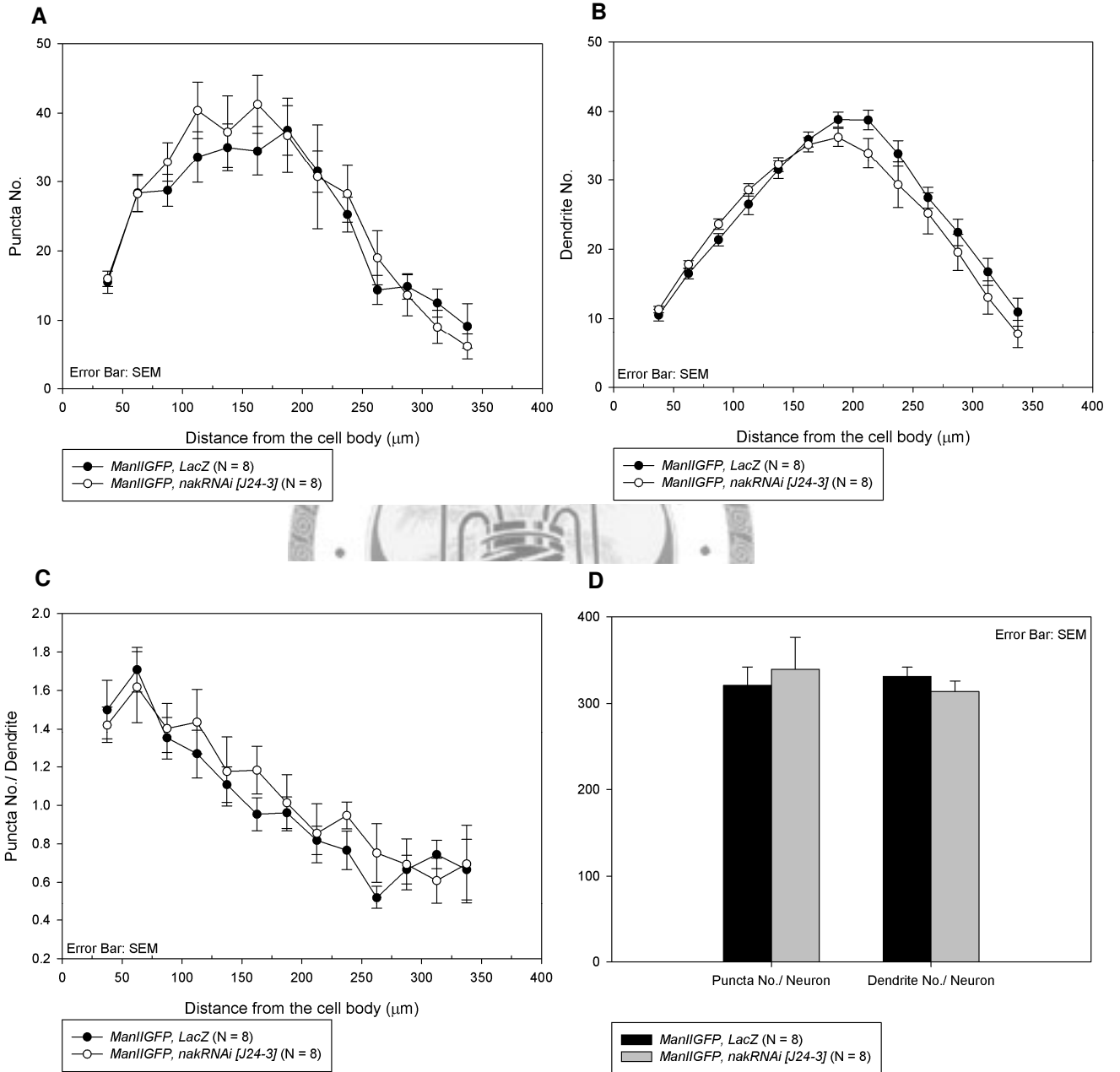


Figure 18. Distribution of Rab4mRFP puncta was not altered by two copies *nak*

RNAi knock-down

109(2)80 > Rab4mRFP, mCD8GFP neurons were co-expressed with two copies LacZ

as control (A-B), or two copies *nak* RNAi (C-D). The single channel images of

Rab4mRFP showed no significant difference (A and C). The dendritic complexity was

simplified in two copies *nak* RNAi knock-down neurons (B and D). Scale bar = 20

μm



Figure. 18

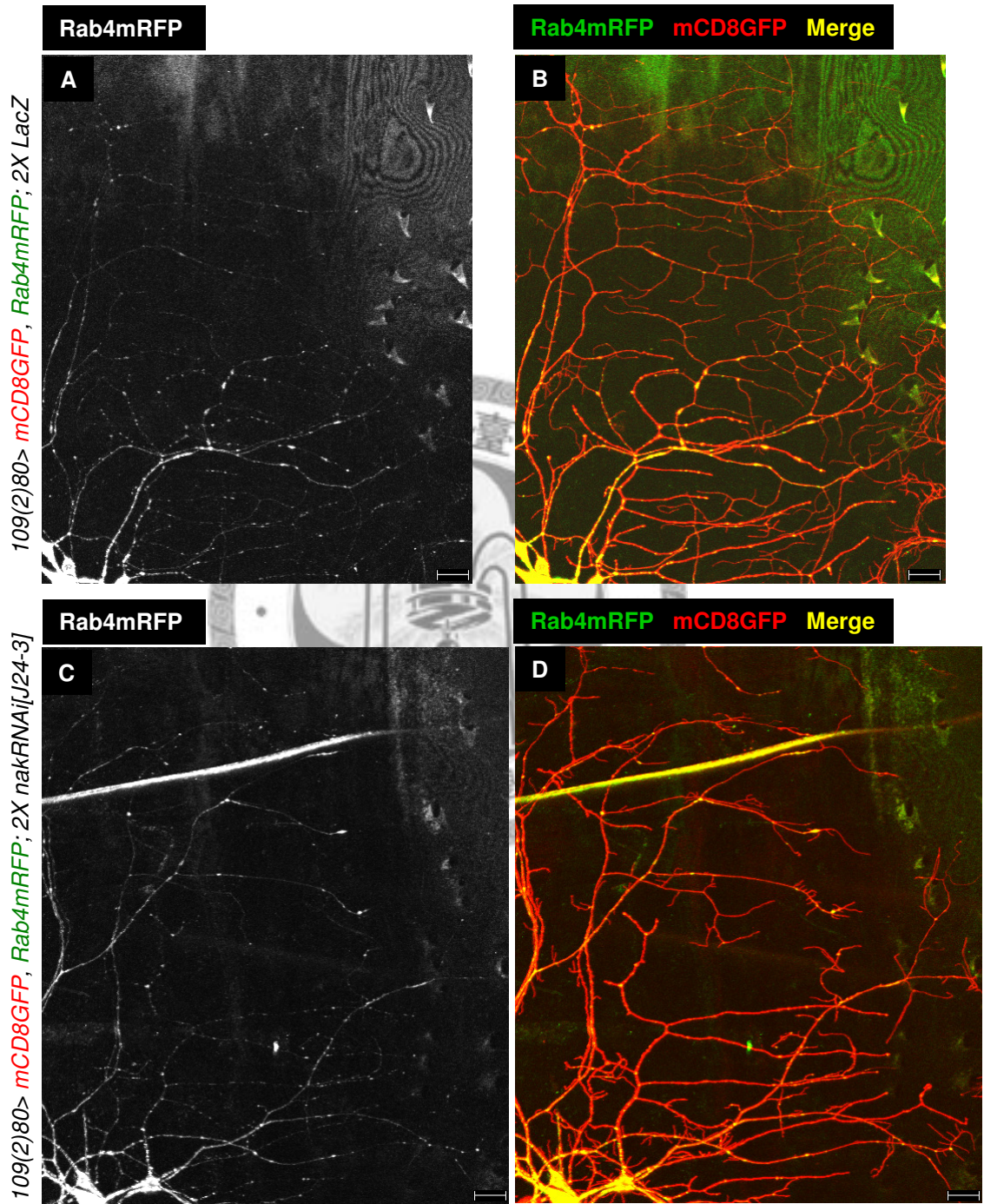


Figure 19. Distribution of Rab4mRFP puncta was not altered by two copies *nak*

RNAi knock-down

This is the statistic results of Rab4mRFP in 2X lacZ control and 2X *nak* RNAi

knock-down da dendrites. (A) Rab4mRFP puncta numbers were plotted against the distance from the cell body. (B) Dendrite numbers were plotted to the distance from soma. (C) The densities of Rab4mRFP were plotted to their distance from soma, the density distributions of Rab4mRFP were not affected by *nak* RNAi expression. (D)

The puncta number and dendrite number of each neuron were summed. The dendrite number/ neuron (right two bars) was reduced in *nak* depleted neurons and the puncta number/ neuron (left two bars) was unaltered.

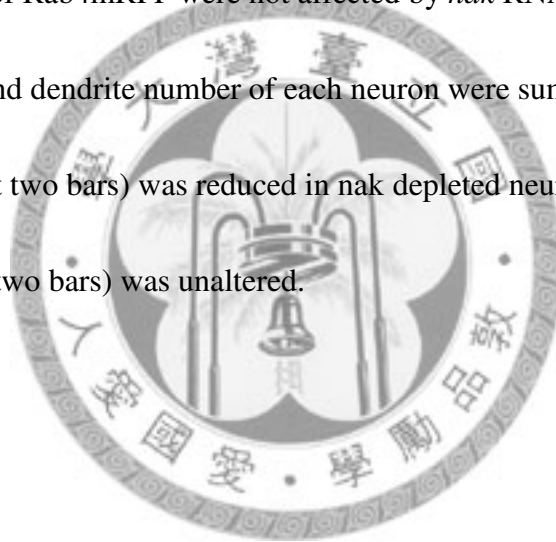


Figure. 19

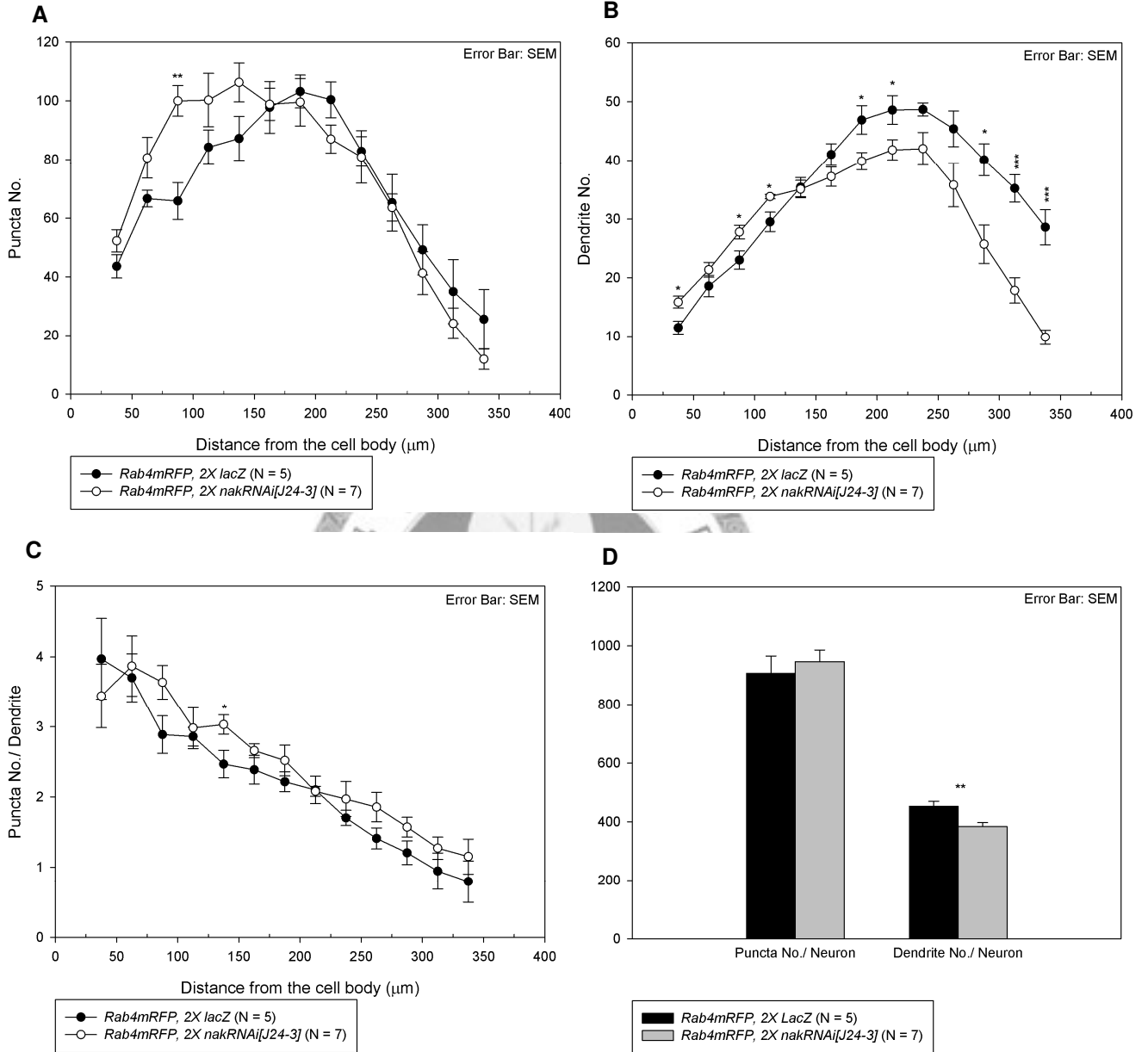


Figure 20. Rab5GFP puncta showed dynamic behavior in dendrites

Rab5GFP monochrome live-image of *109(2)80 > myrmRFP, Rab5GFP* dendrites were shown in 10 sec intervals. Mobile Rab5GFP puncta were marked by arrows, whereas the motionless ones were indicated by arrowheads.



Figure. 20

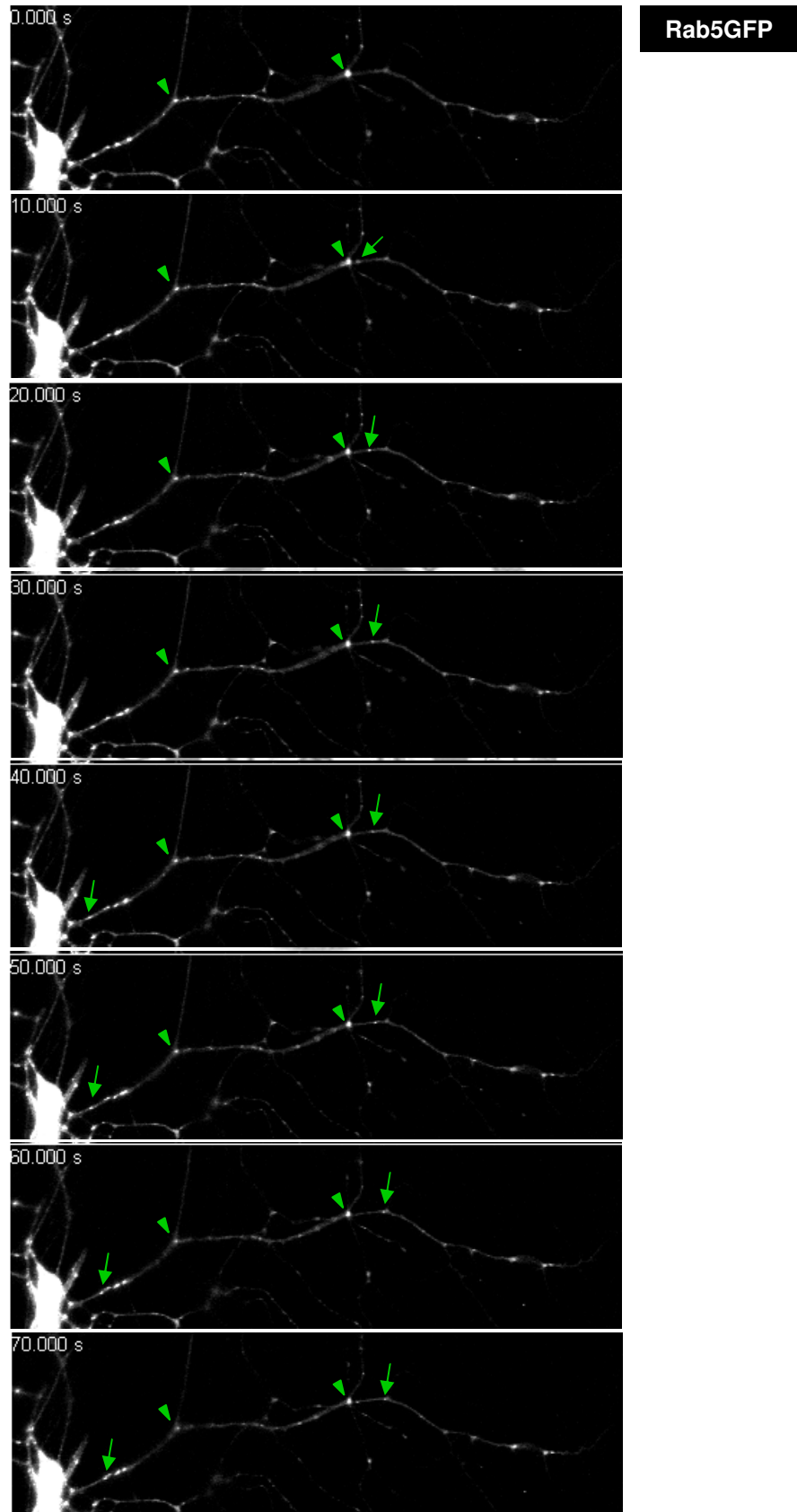


Figure 21. Rab4mRFP puncta displayed local motion in proximal dendrites

Rab4mRFP monochrome live-image of *ppk >Rab4mRFP, mCD8GFP* dendrites were shown in 10 sec intervals. Locally moved Rab4mRFP puncta were marked by arrows, whereas the stationary ones were indicated by arrowheads.



Figure. 21

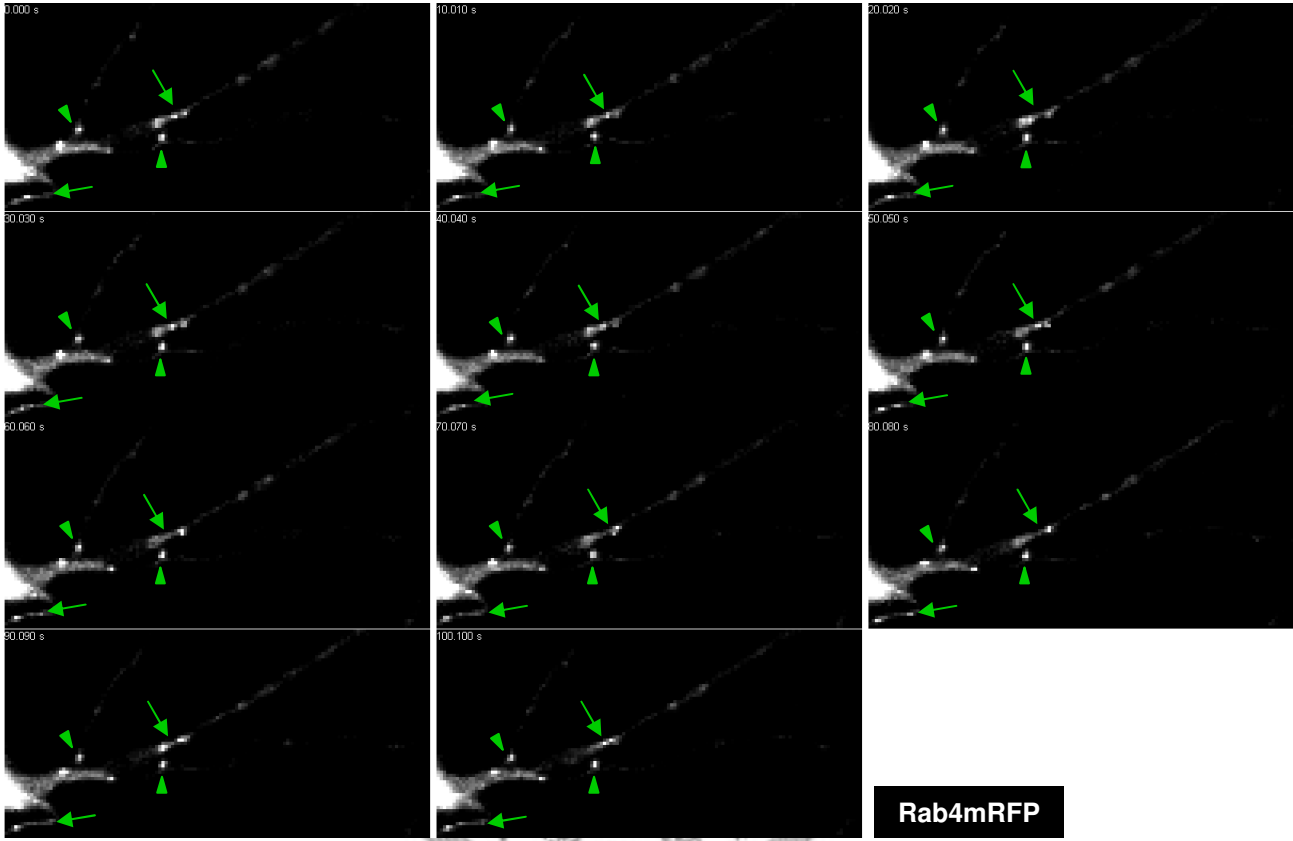
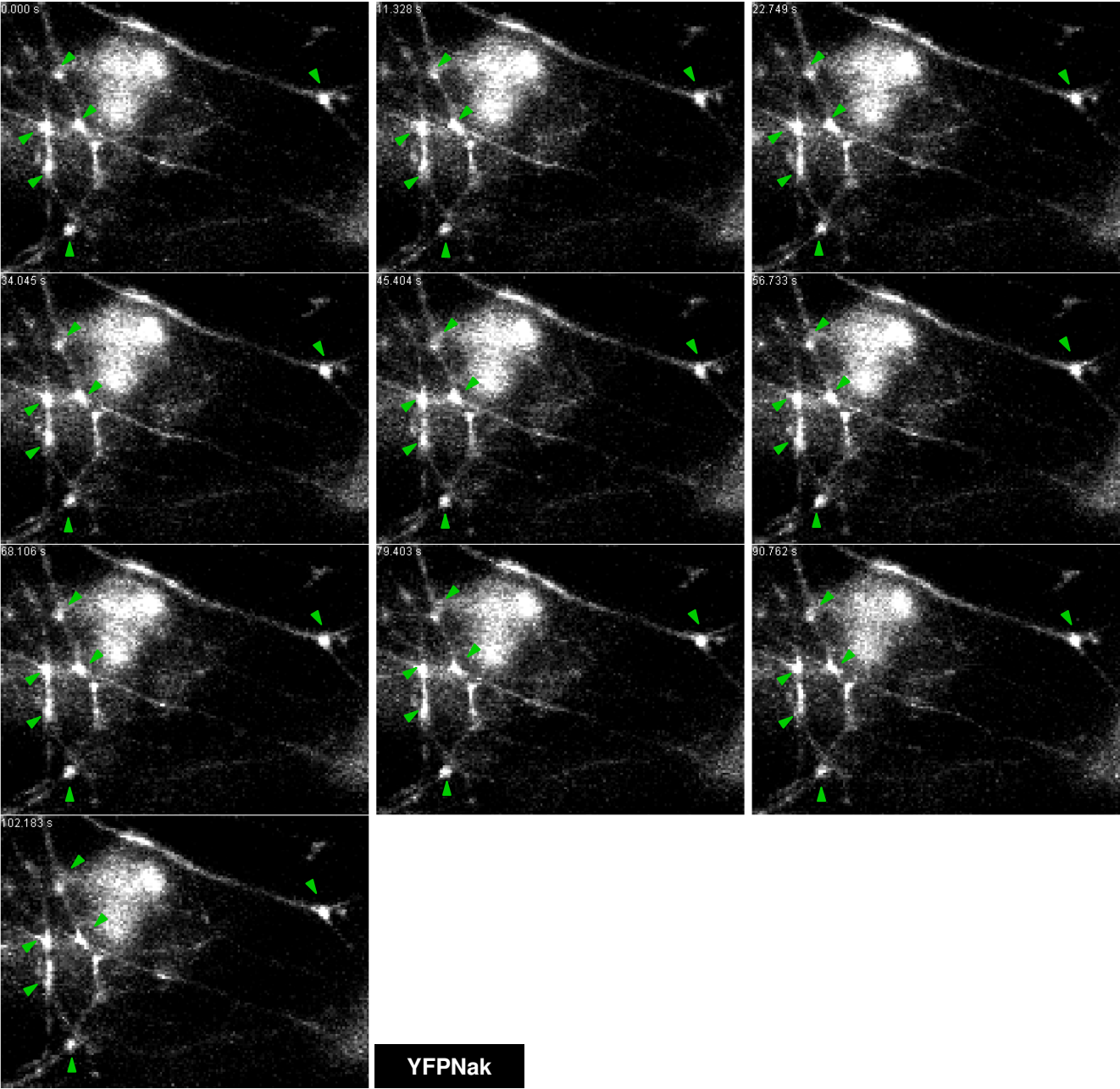


Figure 22. YFPNak puncta displayed static behavior in dendrites

YFPNak monochrome live-image of *109(2)80 > myrmRFP*, *YFPNak* dendrites were shown in about 10 sec intervals. YFPNak puncta were stationary and indicated by arrowheads.



Figure. 22



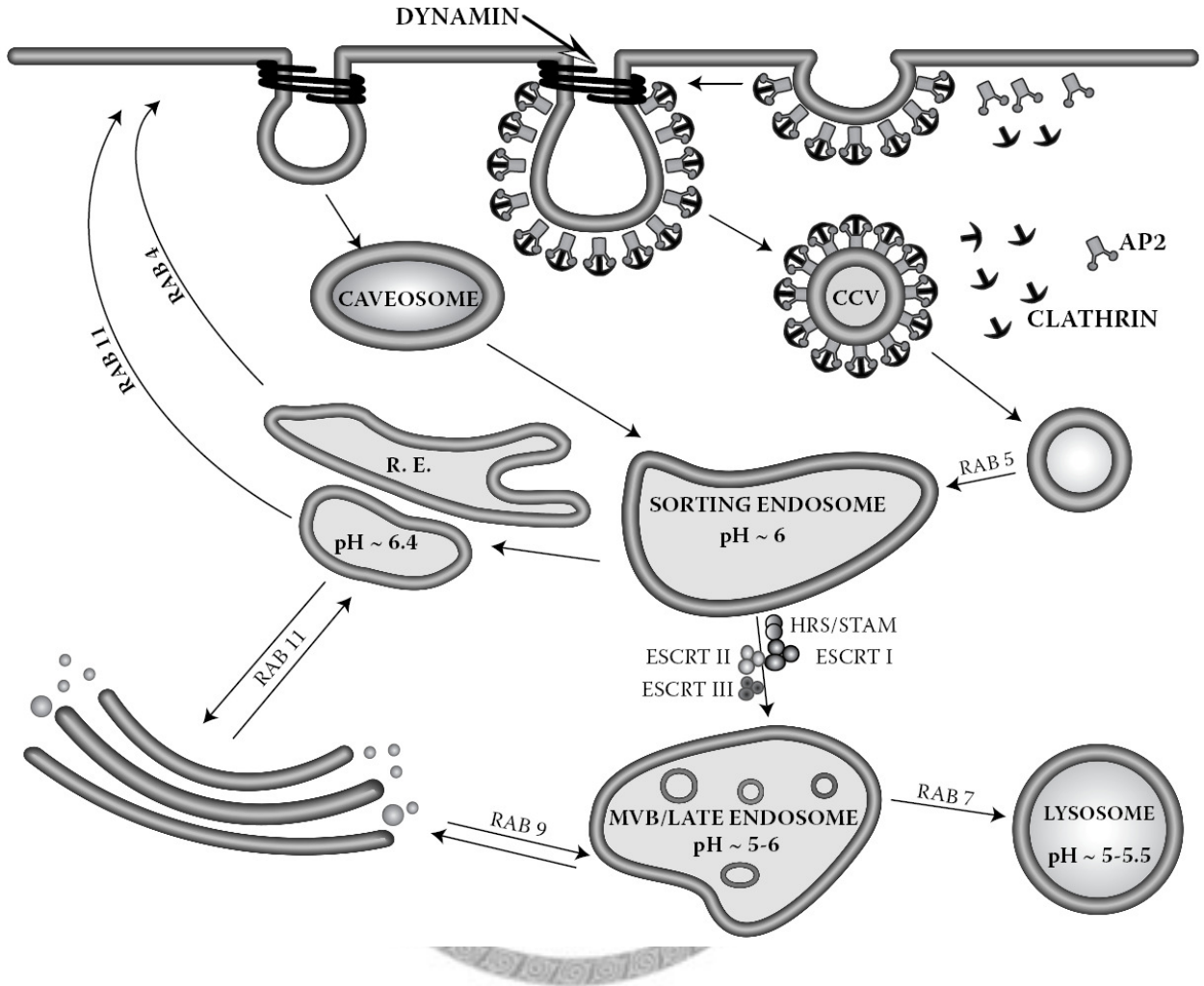
Appendix 1.

Overview of the steps involved in the clathrin mediated endocytic pathway and the role of Rab GTPases

(Taken from “The dynamic synapse” chapter 6 - Studying the Localization, Surface Stability and Endocytosis of Neurotransmitter Receptors by Antibody Labeling and Biotinylation Approaches, 2006, I. Lorena Arancibia-Cárcamo, et al)



Appendix 1



Appendix 2.

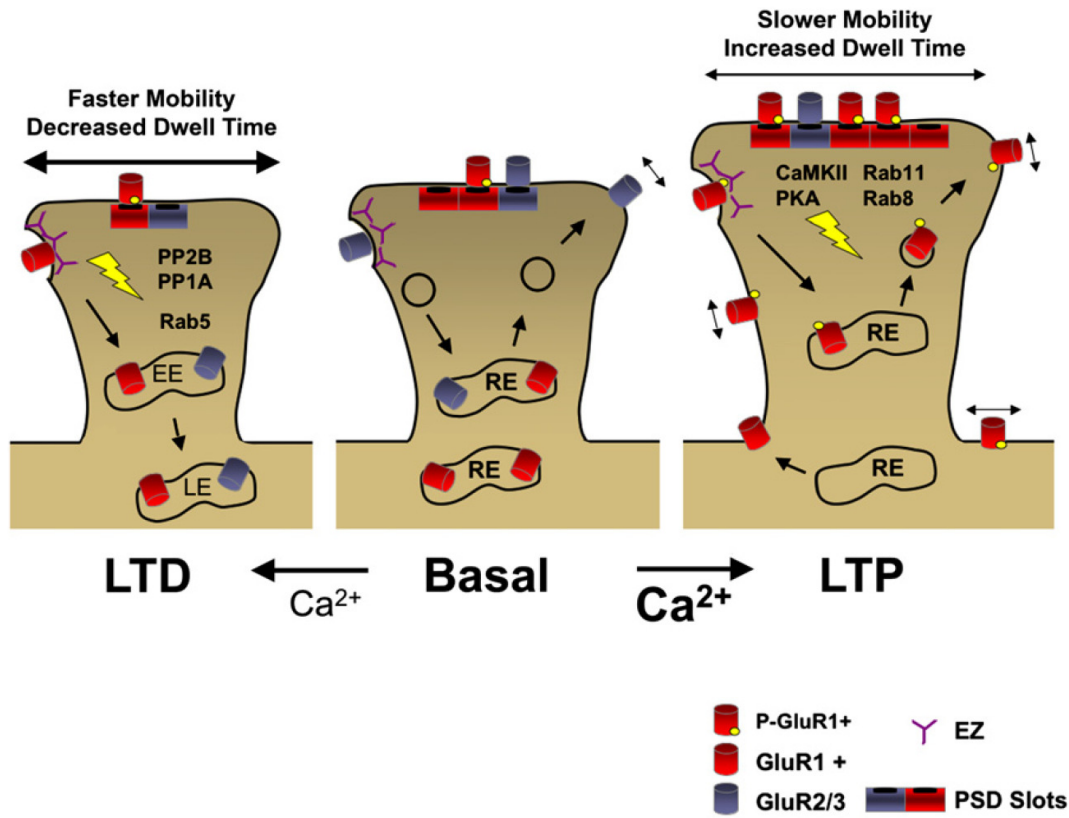
Integrating Models for Receptor Trafficking and Diffusion during Synaptic

Plasticity

(Taken from Newpher, T. M. and M. D. Ehlers (2008). "Glutamate receptor dynamics in dendritic microdomains." Neuron **58**(4): 472-497)



Appendix 2



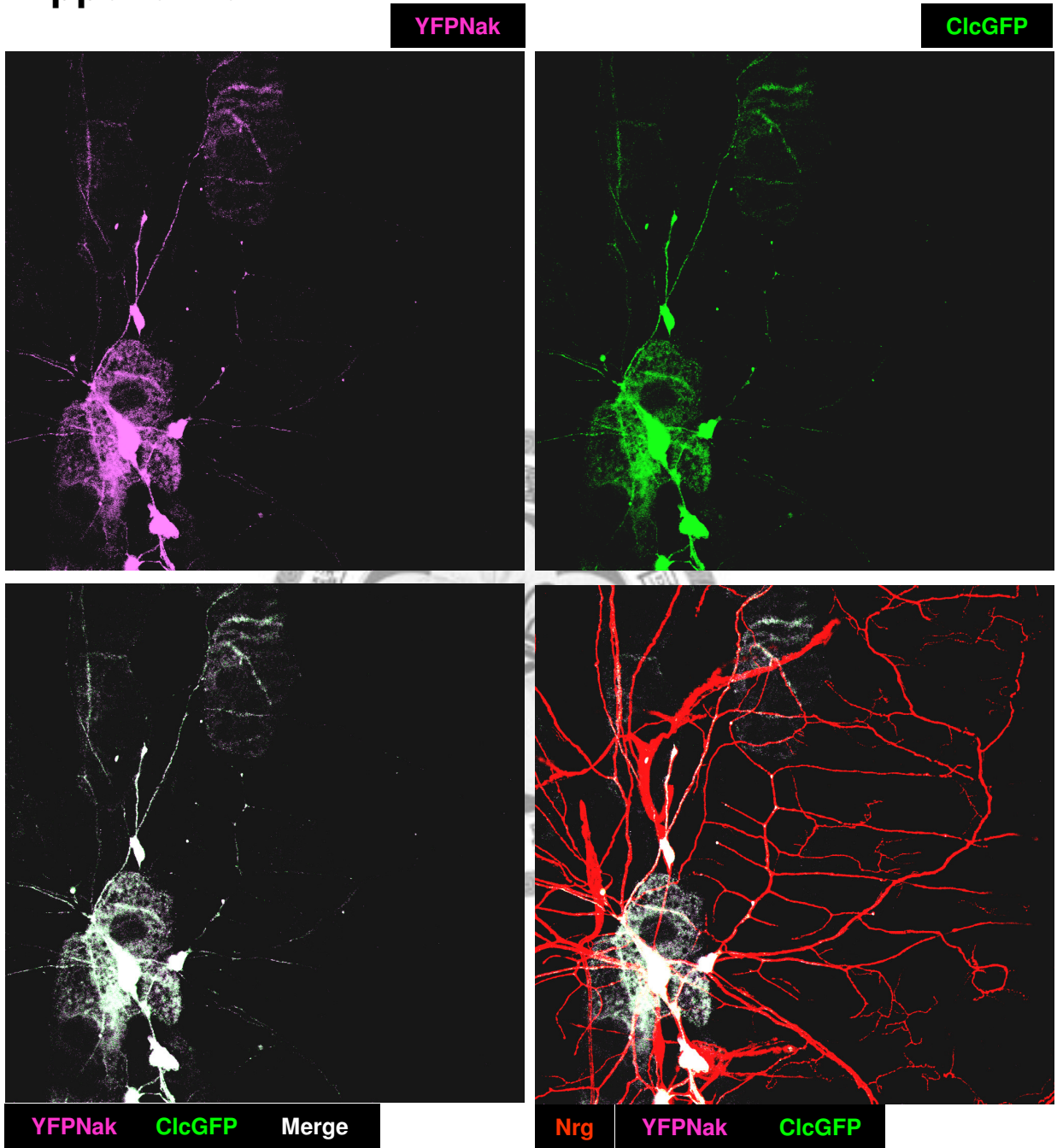
Appendix 3. ClcGFP and YFPNak are well colocalized

(A – D) ClcGFP (green) and YFPNak (magenta) were coexpressed by GAL4109(2)80, Nrg was stained to indicate the dendrite morphology (red). (A) Single channel image showing the distribution of YFPNak. (B) Single channel image showing the distribution of ClcGF. (C-D) Merged images shows good colocalization between YFPNak and ClcGFP

(Images were obtained by Wei-Kan Yang)



Appendix 3



(By Wei-Kan Yang, unpublished)